ruhr.paD
UA Ruhr Zentrum für
partielle Differentialgleichungen

# Parametric Raviart-Thomas elements for mixed methods on domains with curved surfaces

F. Bertrand and G. Starke

Preprint 2016-05

# PARAMETRIC RAVIART-THOMAS ELEMENTS FOR MIXED METHODS ON DOMAINS WITH CURVED SURFACES

FLEURIANNE BERTRAND* AND GERHARD STARKE*

**Abstract.** The finite element approximation on curved boundaries using parametric Raviart-Thomas spaces is studied in the context of the mixed formulation of Poisson's equation as a saddle-point system. It is shown that optimal order convergence is retained on domains with piecewise $C^{k+2}$ boundary for the parametric Raviart-Thomas space of degree $k \geq 0$ under the usual regularity assumptions. This extends the analysis in [3] from the first-order system least squares formulation to mixed approaches of saddle-point type. In addition, a detailed proof of the crucial estimate in three dimensions is given which handles some complications not present in the two-dimensional case. Moreover, the appropriate treatment of inhomogeneous flux boundary conditions is discussed. The results are confirmed by computational results which also demonstrate that optimal order convergence is not achieved, in general, if standard Raviart-Thomas elements are used instead of the parametric spaces.

**Key words.** interpolated boundaries, Raviart-Thomas spaces, parametric finite elements, mixed finite elements

**AMS subject classifications.** 65N30, 65N50

## 1. Introduction.

This paper continues our study of parametric Raviart-Thomas finite elements for domains with curved boundaries which were studied in [3] in the context of first-order system least squares methods. Parametric Raviart-Thomas elements are defined on the basis of the continuous piecewise polynomial mapping known from the isoparametric finite element framework. In the context of mixed variational formulations posed in $H(\mathrm{div}, \Omega)$, they allow a more accurate resolution of flux boundary conditions posed on curved boundary surfaces or curves. The purpose of this paper is to provide a convergence analysis of parametric Raviart-Thomas finite elements on curved domains in the context of the mixed formulation of Poisson's equation. In particular, it will be shown that under sufficient regularity assumptions, the optimal order of convergence is retained on curved domains if a parametric version of Raviart-Thomas elements based on a polynomial mapping is used near the boundary. In the lowest-order case, this result establishes optimal order convergence if a piecewise $C^2$ boundary is interpolated by a polyhedral surface or polygonal curve and the flux boundary conditions are appropriately prescribed on that boundary approximation. Of course, the basis for parametric edge- and face-based elements are the well-known transformation rules with respect to coordinate changes (see, e.g. [17, Sect. 3.9], [6, Sect. 2.1.3]). We will also implicitly make use of connections to exact sequences of parametric edge- and face-based finite element spaces (see e.g. [16]). The framework for the implementation of parametric Raviart-Thomas elements provided in [18] is also related to our work although their focus is on the case of a piecewise affine mapping.

The convergence analysis relies crucially on an estimate for the discrepancy of the normal flux associated with the parametric Raviart-Thomas spaces on the curved boundary if it is set to zero on its piecewise polynomial approximation. This estimate was already proved in [3] for the two-dimensional situation (and even earlier in [4] for the lowest-order case) and is extended here to three dimensions where some additional complications occur. Additionally, the treatment of inhomogeneous flux boundary conditions will be addressed based on a suitable interpolation operator for

*Fakultät für Mathematik, Universität Duisburg-Essen, 45117 Essen, Germany (fleurianne.bertrand@uni-due.de, gerhard.starke@uni-due.de).

the parametric Raviart-Thomas space. This issue should also be of much interest in the context of reconstruction of fluxes or stresses in Raviart-Thomas spaces in the presence of curved boundaries. To this end, the mapping techniques suggested here can be combined with the popular reconstruction or equilibration approaches (cf. [8, 13, 14, 10] and references therein). Due to the lack of optimal order approximation if standard Raviart-Thomas elements (of degree higher than 0) are used instead of the parametric ones, the efficiency of a posteriori error estimators based on such reconstructions is also expected to be deficient.

Clearly, the applicability of parametric Raviart-Thomas spaces is not restricted to Poisson's equation but can be adopted in a straightforward way, e.g., to stress-based mixed methods in elasticity (cf. [6, Chp. 9]). Another important application field is the area of interface problems where curved surfaces arise in a natural way. A promising approach which works in the isoparametric framework for the primal formulation and performs local modifications in the vicinity of the interface was recently studied in [11] and may be worthwhile to pursue in the dual framework with parametric Raviart-Thomas elements. The definition of the parametric Raviart-Thomas elements carries over to other simplicial $H(\mathrm{div})$-conforming spaces like those studied in [6, Sect. 2.3]. For example, for the Brezzi-Douglas-Marini elements $BDM_k$, $k \geq 1$, being a subset of the Raviart-Thomas space $RT_k$, a similar estimate for the normal flux on the curved boundary also holds true. On the other hand, Theorem 5 does not hold if $RT_k$ is replaced by $BDM_k$ since the required approximation order for $\operatorname{div} \mathbf{u}$ is not valid in the polygonal case. We restrict our attention to the RT elements since our focus lies on the optimal-order convergence in $H(\mathrm{div})$ which can be achieved with fewer degrees of freedom than for BDM elements. Parametric $H(\mathrm{curl})$-conforming finite elements may also be examined using the covariant mapping instead of the contravariant one (cf. [6, Sect. 2.1.3], [16], [17, Sect. 3.9]) but the details will be different from our approach, particularly for higher order elements. We also restrict ourselves to simplicial elements since the quadrilateral case is more complicated even without a higher-order parametric mapping (cf. [2]).

In the next section, the parametric Raviart-Thomas finite element spaces needed to approximate fluxes in $H(\mathrm{div}, \Omega)$ with sufficient accuracy will be introduced and its properties, in particular, in connection to mixed methods of saddle-point type will be studied. Section 3 contains an estimate for the normal flux associated with parametric Raviart-Thomas elements on interpolated boundaries which will be crucial for our convergence results. All of this will be described for the three-dimensional case in contrast to the presentation in [3] where a two-dimensional setting was assumed for simplicity. An interpolation operator for parametric finite element spaces will be introduced in Section 4 before all of this is put together to prove optimal order convergence of the saddle-point type mixed method using the parametric Raviart-Thomas spaces in Section 5. The practical issue of handling inhomogeneous flux boundary conditions is treated in Section 6. Finally, computational results illustrating our theoretical findings and demonstrating the necessity of using the parametric variant of the elements are presented.

**2. Parametric Raviart-Thomas finite element spaces.** Throughout this paper, $\Omega \subset \mathbb{R}^d$ $(d = 2, 3)$ will be a bounded domain with Lipschitz continuous and piecewise $C^{k+2}$ boundary $\Gamma = \partial\Omega$ for $k \geq 0$. Optimal order approximation with respect to $H(\mathrm{div}, \Omega)$ is achieved by Raviart-Thomas finite elements on domains with polygonal or polyhedral boundary (see, e.g. [6, Sect. 2.5]). On curved domains, however, this is only true for the lowest-order elements and already fails to hold in

the next-to-lowest-order case. This is similar to the situation with continuous finite elements for $H^1(\Omega)$ approximations where the isoparametric setting is needed if the polynomial degree exceeds one. The same piecewise polynomial approximation of the boundary will be used to define suitable parametric versions of the Raviart-Thomas finite element spaces which retain the optimal order of approximation in the higher-order case.

To this end, $\Omega$ is approximated by a domain $\Omega_h$ which is the image of a polygonal or polyhedral reference domain $\widehat{\Omega}_h$ under a piecewise polynomial mapping of degree $k+1$. In the lowest-order case, $\Omega_h = \widehat{\Omega}_h$ and the standard finite element approach is recovered. Associated with $\Omega_h$ is a triangulation $\mathcal{T}_h$ consisting of elements which are the image of straight triangles or tetrahedra under a polynomial mapping of degree $k+1$. The boundaries of $\Omega_h$ and $\widehat{\Omega}_h$ will be denoted by $\Gamma_h$ and $\widehat{\Gamma}_h$, respectively. Related to the triangulation $\mathcal{T}_h$ of $\Omega_h$ are triangulations $\widetilde{\mathcal{T}}_h$ and $\widehat{\mathcal{T}}_h$ of $\Omega$ and $\widehat{\Omega}_h$, respectively, which have all the vertices in common. For the finite element space $\mathbf{V}_h$, defined with respect to $\mathcal{T}_h$, the polynomial function $\mathbf{v}_h \in \mathbf{V}_h$ may be extended to $\widetilde{T} \in \widetilde{\mathcal{T}}_h$ by using its polynomial representation on the corresponding element $T \in \mathcal{T}_h$. However, $\mathbf{V}_h \not\subseteq H_\Gamma(\mathrm{div}, \Omega)$ (which denotes the subspace of $H(\mathrm{div}, \Omega)$ with vanishing trace of $\mathbf{n} \cdot \mathbf{v}$ on $\Gamma$), in general, since $\mathbf{n} \cdot \mathbf{v}_h$ does not vanish on $\Gamma$ for $\mathbf{v}_h \in \mathbf{V}_h$. Instead, the condition $\mathbf{n}_h \cdot \mathbf{v}_h = 0$ on $\Gamma_h$ is imposed on the space $\mathbf{V}_h$, where $\mathbf{n}_h$ is the outward normal with respect to $\Gamma_h$. It is necessary to keep track of the effect that this inexactness of the boundary condition has on the overall accuracy of our finite element approximation.

For the sake of simplicity, the assumption is made that the triangulation $\widetilde{\mathcal{T}}_h$ of $\Omega$ is such that each boundary side (edge or face, respectively, in two or three dimensions) of elements in $\widetilde{\mathcal{T}}_h$ is completely contained in one of the $C^{k+2}$ patches of $\Gamma$. Moreover, we restrict ourselves to the situation that each element $\widetilde{T} \in \widetilde{\mathcal{T}}_h$ has at most one curved side. This assumption is also reasonable from a practical point of view and can always be achieved by an additional refinement step.

The piecewise polynomial mapping of degree $k+1$ from $\widehat{\Omega}_h$ to $\Omega_h$ is denoted by $F_h$ and coincides with the one used in the isoparametric finite element framework (see e.g. [7, Sect. 10.4]). For $k > 0$, the piecewise polynomial mapping $F_h$ differs from the identity map only on triangles adjacent to curved boundary edges. Under our assumptions on the smoothness of $\Gamma$, the distance between $\Gamma_h = F_h(\widehat{\Gamma}_h)$ and $\Gamma = \partial\Omega$ is of the order $h^{k+2}$ (see [7, Sect. 4.7]). Moreover, the Jacobian $J_{F_h}$ of the mapping $F_h$ satisfies $\|J_{F_h}\|_{W^{k+1}_\infty(\widehat{\Omega}_h)} \le C$ with a constant $C$ which is independent of $h$. For sufficiently small $h$, the mapping $F_h$ is invertible and $\|J^{-1}_{F_h}\|_{W^{k+1}_\infty(\Omega_h)} \le C$ holds for the associated Jacobian (cf. [7, Sect. 4.7], [15]).

The standard Raviart-Thomas space of degree $k \ge 0$ with respect to the triangulation $\widehat{\mathcal{T}}_h$ of a polyhedrally bounded domain $\widehat{\Omega}_h$ is given by

$$\widehat{\mathbf{V}}_h^k = \{\mathbf{v}_h \in H(\mathrm{div}, \widehat{\Omega}_h) : \mathbf{v}_h|_{\widehat{T}} = \begin{pmatrix} p_k(\widehat{\mathbf{x}}) \\ q_k(\widehat{\mathbf{x}}) \\ r_k(\widehat{\mathbf{x}}) \end{pmatrix} + \begin{pmatrix} \hat{x}_1 \\ \hat{x}_2 \\ \hat{x}_3 \end{pmatrix} s_k(\widehat{\mathbf{x}})\} \tag{1}$$

with polynomials $p_k$, $q_k$, $r_k$ and $s_k$ of degree $k$. Based on this, the parametric Raviart-Thomas space is defined as

$$\mathbf{V}_h^k = \{\mathbf{v}_h : \Omega_h \to \mathbb{R}^3 : \mathbf{v}_h(\mathbf{x}) = \frac{1}{\det J_{F_h}(\widehat{\mathbf{x}})} J_{F_h}(\widehat{\mathbf{x}}) \widehat{\mathbf{v}}_h(\widehat{\mathbf{x}}) \text{ with } \widehat{\mathbf{v}}_h \in \widehat{\mathbf{V}}_h^k\}\,, \tag{2}$$

with $\mathbf{x} = F_h(\widehat{\mathbf{x}})$ where $\widehat{\mathbf{V}}_h^k$ denotes the standard Raviart-Thomas finite element space.

It is worth mentioning that the transformation in (2) is in fact the contravariant Piola mapping for the transformation of vector fields (see e.g. [18], [6, Sect. 2.1.3]). We also introduce the subspaces

$$\begin{aligned} \widehat{\mathbf{V}}_{h,0}^k &= \{\mathbf{v}_h \in \widehat{\mathbf{V}}_h^k : \widehat{\mathbf{n}}_h \cdot \widehat{\mathbf{v}}_h = 0 \text{ on } \widehat{\Gamma}_h\}\,, \\ \mathbf{V}_{h,0}^k &= \{\mathbf{v}_h \in \mathbf{V}_h^k : \mathbf{n}_h \cdot \mathbf{v}_h = 0 \text{ on } \Gamma_h\}\,. \end{aligned} \tag{3}$$

This is motivated by the fact that $\widehat{\mathbf{V}}_{h,0}^k \subset H_{\widehat{\Gamma}_h}(\mathrm{div}, \widehat{\Omega}_h)$ ensures $\mathbf{V}_{h,0}^k \subset H_{\Gamma_h}(\mathrm{div}, \Omega_h)$ (see [6, Sect. 2.1.3]). More precisely, (2) leads to

$$(\mathrm{div}\ \mathbf{v}_h)(F_h(\widehat{\mathbf{x}})) = \frac{1}{\det J_{F_h}(\widehat{\mathbf{x}})}(\widehat{\mathrm{div}}\ \widehat{\mathbf{v}}_h)(\widehat{\mathbf{x}}) \text{ for all } \widehat{\mathbf{x}} \in \widehat{\Omega}_h \tag{4}$$

(where $\widehat{\mathrm{div}}$ denotes differentiation with respect to $\widehat{\mathbf{x}}$) and that $\widehat{\mathbf{n}}_h \cdot \widehat{\mathbf{v}}_h = 0$ on $\widehat{\Gamma}_h$ is equivalent to $\mathbf{n}_h \cdot \mathbf{v}_h = 0$ on $\Gamma_h$. Of course, $\mathbf{V}_h^0 = \widehat{\mathbf{V}}_h^0$ holds in the lowest-order case. As approximation space for the pressure, the standard space of piecewise, possibly discontinuous, polynomials of degree $k$, combined with the parametric mapping,

$$S_h^k = \{\widehat{q}_h \circ F_h^{-1} : \Omega_h \to \mathbb{R}^3 : \widehat{q}_h|_T \text{ polynomial of degree } k\}\,, \tag{5}$$

is used which may be regarded as a subspace of $L^2(\Omega_h)$, $L^2(\widehat{\Omega}_h)$ or $L^2(\Omega)$.

Concerning the implementation of parametric Raviart-Thomas elements, some remarks seem to be appropriate at this point. The usual way for setting up the variational problem in the discrete spaces consists in the use of quadrature rules which are exact for all polynomials of a certain degree on the individual elements. For standard isoparametric finite elements that degree of exactness is then inherited simply by appropriately mapping the quadrature points. This is not possible, however, for the parametric Raviart-Thomas elements since the function $J_{F_h}(\widehat{\mathbf{x}})\widehat{\mathbf{v}}_h(\widehat{\mathbf{x}})/\det J_{F_h}(\widehat{\mathbf{x}})$ on the reference element is no longer polynomial. On the other hand, $J_{F_h}$ is close to the identity (cf. [7, Sect. 10.4] and [15, Prop. 2]) and therefore the quadrature error is usually marginal under practical circumstances (cf. also [9, Sect. 4.4, particularly Remark 4.4.3]). The effect of numerical quadrature on the finite element approximation can then be controlled in the usual way by viewing this as a variational crime (see [9, Theorem 4.4.1]).

**3. An estimate for the normal flux on interpolated boundaries.** Throughout this section, the subspace $\mathbf{V}_{h,0}^k$ of parametric Raviart-Thomas elements on $\mathcal{T}_h$ with boundary conditions $\mathbf{n}_h \cdot \mathbf{v}_h = 0$ on $\Gamma_h$ is considered. As already discussed, $\mathbf{V}_{h,0}^k$ is not a subspace of $H_\Gamma(\mathrm{div}, \Omega)$, in general, for a curved boundary $\Gamma = \partial\Omega$. In other words, the use of parametric Raviart-Thomas elements on a domain with curved boundary constitutes a variational crime, in general, in analogy to the standard isoparametric case [7, Sect. 10.4]. For the purpose of controlling the effect that the inexactness of the boundary representation has on the error associated with the finite element approximation, an estimate for the approximated normal flux $\mathbf{n} \cdot \mathbf{v}_h$ on $\Gamma$ for $\mathbf{v}_h \in \mathbf{V}_{h,0}^k$ is needed. We will use the following common shorthand notation: $a(\xi) \gtrsim b(\xi)$ stands for the existence of a constant $C > 0$ which is independent of the parameters involved (in our case, the local or global mesh-size $h_T$ or $h$, respectively) such that $a(\xi) \geq Cb(\xi)$ holds for all admissible $\xi$. Moreover, $a(\xi) \eqsim b(\xi)$ stands for both $a(\xi) \gtrsim b(\xi)$ and $b(\xi) \gtrsim a(\xi)$ to be satisfied. Norm estimates of the form

$$\|\mathbf{v}_h\|_{0,T}^2 \gtrsim h_T \|\mathbf{v}_h\|_{0,\partial T}^2\,,\ \|\mathrm{div}\ \mathbf{v}_h\|_{0,T}^2 \gtrsim h_T \|\mathrm{div}\ \mathbf{v}_h\|_{0,\partial T}^2 \tag{6}$$

which hold for all $\mathbf{v}_h \in \mathbf{V}_h^k$ will be used repeatedly. Similarly, the norm equivalences

$$\|\mathbf{v}_h\|_{0,\Omega_h}^2 \eqsim \|\mathbf{v}_h\|_{0,\Omega}^2 \,, \|\operatorname{div} \mathbf{v}_h\|_{0,\Omega_h}^2 \eqsim \|\operatorname{div} \mathbf{v}_h\|_{0,\Omega}^2 \tag{7}$$

hold for all $\mathbf{v}_h \in \mathbf{V}_h^k$ if $\Omega_h$ is sufficiently close to $\Omega$ such that it admits an invertible mapping between $\Omega_h$ and $\Omega$. Such a mapping will be introduced and used in the proof of Theorem 5.1 in Section 4 and is a standard tool in the context of isoparametric finite elements (cf. [7, Sect. 10.4] and [15]).

The following estimate lies at the heart of our convergence analysis of the parametric Raviart-Thomas method.

THEOREM 1. *Assume that $\Gamma = \partial\Omega$ is a piecewise $C^{k+2}$ boundary, $k \geq 0$, and that the triangulation $\mathcal{T}_h$ is such that no boundary side of elements in $\mathcal{T}_h$ belongs to more than one of the $C^{k+2}$ patches of $\Gamma$. Then, for any $\alpha > 1/2$,*

$$|\langle \mathbf{n} \cdot \mathbf{v}_h, q \rangle_{0,\Gamma}| \lesssim h^{k+1} \|\mathbf{v}_h\|_{\operatorname{div},\Omega} \|q\|_{\alpha,\Gamma} \tag{8}$$

*holds for all $\mathbf{v}_h \in \mathbf{V}_{h,0}^k$ and $q \in H^\alpha(\Gamma)$.*

In the two-dimensional case, one can actually set $\alpha = 1/2$ in Theorem 1 as we already proved in [3, Thm. 3.1]. However, for our purpose in Section 5, the above statement suffices. In fact, we could even set $\alpha = 3/2$ under our regularity assumptions in Section 5. Since the three-dimensional case contains some additional complications, we will present a complete proof below.

*Proof.* Let us consider a fixed curved boundary face $\Gamma_T \subset \Gamma$ and the adjacent tetrahedron $\widetilde{T} \in \widetilde{\mathcal{T}}_h$. By $\gamma^0 T$ and $\gamma^0 \widehat{T}$ we denote the corresponding boundary faces of $T \in \mathcal{T}_h$ and $\widehat{T} \in \widehat{\mathcal{T}}_h$, respectively. For the fixed curved boundary face $\Gamma_T \subset \Gamma$ with adjacent tetrahedron $\widetilde{T} \in \widetilde{\mathcal{T}}_h$, we need in addition the curved triangle $\widehat{\Gamma}_T = F_h^{-1}(\Gamma_T)$ and adjacent tetrahedron $\breve{T} = F_h^{-1}(\widetilde{T})$. The corresponding parametric face $\gamma^0 T \subset \Gamma_h$ is, by definition, mapped onto the straight face $\gamma^0 \widehat{T} = F_h^{-1}(\gamma^0 T)$ with its adjacent

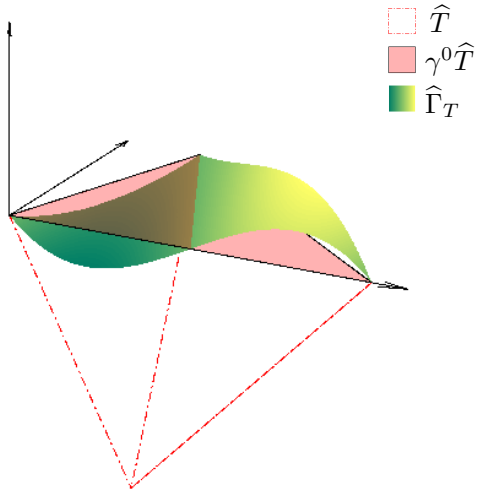


FIG. 1. *Notations for curved surface triangles*

triangle $\widehat{T} = F^{-1}(T)$. The coordinate system may be shifted and rotated in such a way that the straight face $\gamma^0\widehat{T}$ is located on the $(x_1, x_2)$-plane and the longest edge of $\gamma^0\widehat{T}$ on the interval $[0, h_T]$ of the $x_1$ axis (see Figure 1). With respect to these coordinates, $\widehat{\Gamma}_T$ may then be parametrized as

$$\widehat{\Gamma}_T = \left\{ \begin{pmatrix} \boldsymbol{\xi} \\ \eta(\boldsymbol{\xi}) \end{pmatrix} \ : \ \boldsymbol{\xi} \in \gamma^0\widehat{T} \right\} . \tag{9}$$

When it is convenient, we will also denote by $\widetilde{\boldsymbol{\xi}}$ the point on the surface parametrized with $\boldsymbol{\xi}$, i.e. $\widetilde{\boldsymbol{\xi}} = (\boldsymbol{\xi}, \eta(\boldsymbol{\xi}))^\top$. Following the standard construction associated with isoparametric finite elements (cf. [15]), we have that $\eta(\boldsymbol{\xi})$ does in fact vanish for all points in the set

$$\mathcal{N} = \{(h\frac{j}{k} + \breve{P}_1\frac{i}{k}, \breve{P}_2\frac{i}{k}) \ : \ 0 \le j \le k - i, 0 \le i \le k)\} , \tag{10}$$

where $(\breve{P}_1, \breve{P}_2)$ denotes the vertex of $\gamma^0\widehat{T}$ opposite to the longest edge (located on the $x_1$-axis). This implies for all $\boldsymbol{\xi} \in \gamma^0\widehat{T}$ that

$$|\nabla\eta(\boldsymbol{\xi})| \lesssim h_T^{k+1} \text{ and } |\eta(\boldsymbol{\xi})| \lesssim h_T^{k+2} \tag{11}$$

holds. Since, by construction, $\widehat{\mathbf{n}} \cdot \widehat{\mathbf{v}}_h = 0$ on $\gamma^0\widehat{T}$, the functions in the Raviart-Thomas space of degree $k$ are of the form

$$\widehat{\mathbf{v}}_h(\widehat{\mathbf{x}}) = \begin{pmatrix} \boldsymbol{\alpha}_k(\widehat{\mathbf{x}}) \\ 0 \end{pmatrix} + \begin{pmatrix} \boldsymbol{\beta}_k(\widehat{\mathbf{x}}) \\ \gamma_k(\widehat{\mathbf{x}}) \end{pmatrix} \cdot \widehat{\mathbf{x}} =: \begin{pmatrix} \widehat{\mathbf{w}}_h(\widehat{\mathbf{x}}) \\ \hat{x}_3\gamma_k(\widehat{\mathbf{x}}) \end{pmatrix} \tag{12}$$

with a scalar polynomial $\gamma_k$ and two-dimensional polynomials $\boldsymbol{\alpha}_k$ and $\boldsymbol{\beta}_k$ of degree $k$. This implies, that on $\widehat{\Gamma}_T$ (with normal direction $\widehat{\mathbf{n}}$),

$$\widehat{\mathbf{n}} \cdot \widehat{\mathbf{v}}_h = \frac{1}{(1 + |\nabla\eta(\boldsymbol{\xi})|^2)^{1/2}} \left( -\nabla\eta(\boldsymbol{\xi}) \cdot \widehat{\mathbf{w}}_h(\widetilde{\boldsymbol{\xi}}) + \gamma_k(\widetilde{\boldsymbol{\xi}})\eta(\boldsymbol{\xi}) \right) \tag{13}$$

holds which, for $q \in L^2(\widehat{\Gamma}_T)$, leads to

$$\langle \widehat{\mathbf{n}} \cdot \widehat{\mathbf{v}}_h, q \rangle_{0,\widehat{\Gamma}_T} = \int_{\gamma^0\widehat{T}} \left( -\nabla\eta(\boldsymbol{\xi}) \cdot \widehat{\mathbf{w}}_h(\tilde{\boldsymbol{\xi}}) + \gamma_k(\tilde{\boldsymbol{\xi}})\eta(\boldsymbol{\xi}) \right) q(\widetilde{\boldsymbol{\xi}}) \, \mathrm{d}\boldsymbol{\xi} . \tag{14}$$

From $(\widehat{\mathbf{v}}_h)_3(\widetilde{\boldsymbol{\xi}}) = \eta(\boldsymbol{\xi})\gamma_k(\widetilde{\boldsymbol{\xi}})$ we deduce that

$$\partial_3^{l+1}(\widehat{\mathbf{v}}_h)_3(\boldsymbol{\xi}, 0) = (l+1)\partial_3^l\gamma_k(\boldsymbol{\xi}, 0) \ , \ l = 0, 1, ..., k . \tag{15}$$

and therefore

$$\begin{aligned} \eta(\boldsymbol{\xi})\gamma_k(\widetilde{\boldsymbol{\xi}}) &= \eta(\boldsymbol{\xi}) \sum_{l=0}^{k} \frac{\partial_3^l\gamma_k(\boldsymbol{\xi}, 0)}{l!} \left(\eta(\boldsymbol{\xi})\right)^l \\ &= \sum_{l=0}^{k} \frac{\partial_3^{l+1}(\widehat{\mathbf{v}}_h)_3(\boldsymbol{\xi}, 0)}{(l+1)!} \left(\eta(\boldsymbol{\xi})\right)^{l+1} = \sum_{l=1}^{k+1} \frac{\partial_3^l(\widehat{\mathbf{v}}_h)_3(\boldsymbol{\xi}, 0)}{l!} \left(\eta(\boldsymbol{\xi})\right)^l . \end{aligned} \tag{16}$$

Using the Cauchy-Schwarz inequality and (11), it follows from (14) that

$$\begin{aligned}\langle \widehat{\mathbf{n}} \cdot \widehat{\mathbf{v}}_h, q\rangle_{0,\widehat{\Gamma}_T} &\leq \left[\left(\int_{\gamma^0\widehat{T}} \left(-\nabla\eta(\boldsymbol{\xi})\cdot\widehat{\mathbf{w}}_h(\widetilde{\boldsymbol{\xi}})\right)^2 \,\mathrm{d}\boldsymbol{\xi}\right)^{1/2} + \left(\int_{\gamma^0\widehat{T}} \gamma_k(\widetilde{\boldsymbol{\xi}})^2\eta(\boldsymbol{\xi})^2 \,\mathrm{d}\boldsymbol{\xi}\right)^{1/2}\right] \\ &\qquad \left(\int_{\gamma^0\widehat{T}} q(\widetilde{\boldsymbol{\xi}})^2 \,\mathrm{d}\boldsymbol{\xi}\right)^{1/2} \\ &\lesssim \left[h_T^{k+1}\left(\int_{\gamma^0\widehat{T}} |\widehat{\mathbf{w}}_h(\widetilde{\boldsymbol{\xi}})|^2 \,\mathrm{d}\boldsymbol{\xi}\right)^{1/2} \right. \\ &\qquad \left. + \left(\int_{\gamma^0\widehat{T}} \sum_{l=1}^{k+1} (\partial_3^l(\widehat{\mathbf{v}}_h)_3(\boldsymbol{\xi},0))^2 h_T^{2l(k+2)} \,\mathrm{d}\boldsymbol{\xi}\right)^{1/2}\right] \|q\|_{0,\widehat{\Gamma}_T} \\ &\lesssim \left[h_T^{k+1}\|\widehat{\mathbf{w}}_h\|_{0,\widehat{\Gamma}_T} + \sum_{l=1}^{k+1} h_T^{l(k+2)}\|\partial_3^l(\widehat{\mathbf{v}}_h)_3\|_{0,\gamma_0\widehat{T}}\right]\|q\|_{0,\widehat{\Gamma}_T}\end{aligned}$$

holds. Using (6) and inverse estimates (cf. [7, Lem. 4.5.3]) this turns into

$$\begin{aligned}\langle \widehat{\mathbf{n}} \cdot \widehat{\mathbf{v}}_h, q\rangle_{0,\widehat{\Gamma}_T} &\lesssim \left[h_T^{k+1/2}\left(\|(\widehat{\mathbf{v}}_h)_1\|_{0,\widehat{T}} + \|(\widehat{\mathbf{v}}_h)_2\|_{0,\widehat{T}}\right)\right. \\ &\qquad \left. + \sum_{l=1}^{k+1} h_T^{l(k+2)-1/2}\|\partial_3^l(\widehat{\mathbf{v}}_h)_3\|_{0,\widehat{T}}\right]\|q\|_{0,\widehat{\Gamma}_T} \\ &\lesssim h_T^{k+1/2}\|\widehat{\mathbf{v}}_h\|_{0,\widehat{T}}\|q\|_{0,\widehat{\Gamma}_T}\,,\end{aligned} \tag{17}$$

which etablishes the desired bound with respect to $L^2(\widehat{\Gamma}_T)$.

Starting again from (14) and integrating by parts,

$$\begin{aligned}\langle \widehat{\mathbf{n}} \cdot \widehat{\mathbf{v}}_h, q\rangle_{0,\widehat{\Gamma}_T} &= \int_{\gamma^0\widehat{T}} \left(-\nabla\eta(\boldsymbol{\xi})\cdot\widehat{\mathbf{w}}_h(\widetilde{\boldsymbol{\xi}})\right) q(\widetilde{\boldsymbol{\xi}}) + \gamma_k(\widetilde{\boldsymbol{\xi}})\eta(\boldsymbol{\xi})q(\widetilde{\boldsymbol{\xi}}) \,\mathrm{d}\boldsymbol{\xi} \\ &= \int_{\gamma^0\widehat{T}} \eta(\boldsymbol{\xi})\,\mathrm{div}(\widehat{\mathbf{w}}_h(\widetilde{\boldsymbol{\xi}})q(\widetilde{\boldsymbol{\xi}})) + \gamma_k(\widetilde{\boldsymbol{\xi}})\eta(\boldsymbol{\xi})q(\widetilde{\boldsymbol{\xi}}) \,\mathrm{d}\boldsymbol{\xi} \\ &\qquad - \int_{\partial(\gamma^0\widehat{T})} \eta(\boldsymbol{\xi})q(\widetilde{\boldsymbol{\xi}})\left(\mathbf{n}_{\gamma^0\widehat{T}}\cdot\widehat{\mathbf{w}}_h(\widetilde{\boldsymbol{\xi}})\right) \,\mathrm{d}\boldsymbol{\xi} \\ &= \int_{\gamma^0\widehat{T}} \eta(\boldsymbol{\xi})\left(q(\widetilde{\boldsymbol{\xi}})\left(\mathrm{div}\,\widehat{\mathbf{w}}_h(\widetilde{\boldsymbol{\xi}}) + \gamma_k(\widetilde{\boldsymbol{\xi}})\right) + \widehat{\mathbf{w}}_h(\widetilde{\boldsymbol{\xi}})\cdot\nabla q(\widetilde{\boldsymbol{\xi}})\right) \,\mathrm{d}\boldsymbol{\xi} \\ &\qquad - \int_{\partial(\gamma^0\widehat{T})} \eta(\boldsymbol{\xi})q(\widetilde{\boldsymbol{\xi}})\left(\mathbf{n}_{\gamma^0\widehat{T}}\cdot\widehat{\mathbf{w}}_h(\widetilde{\boldsymbol{\xi}})\right) \,\mathrm{d}\boldsymbol{\xi}\end{aligned}$$

is obtained, from which by using the Cauchy-Schwarz inequality and (11),

$$\begin{aligned}\langle \widehat{\mathbf{n}} \cdot \widehat{\mathbf{v}}_h, q\rangle_{0,\widehat{\Gamma}_T} &\leq \left(\int_{\gamma^0\widehat{T}} \eta(\boldsymbol{\xi})^2\left(\mathrm{div}\,\widehat{\mathbf{w}}_h(\widetilde{\boldsymbol{\xi}}) + \gamma_k(\widetilde{\boldsymbol{\xi}})\right)^2 \,\mathrm{d}\boldsymbol{\xi}\right)^{1/2}\|q\|_{0,\widehat{\Gamma}_T} \\ &\qquad + \left(\int_{\gamma^0\widehat{T}} \eta(\boldsymbol{\xi})^2|\widehat{\mathbf{w}}_h(\widetilde{\boldsymbol{\xi}})|^2 \,\mathrm{d}\boldsymbol{\xi}\right)^{1/2}|q|_{1,\widehat{\Gamma}_T} \\ &\qquad + \left|\int_{\partial(\gamma^0\widehat{T})} \eta(\boldsymbol{\xi})q(\widetilde{\boldsymbol{\xi}})\left(\mathbf{n}_{\gamma^0\widehat{T}}\cdot\widehat{\mathbf{w}}_h(\widetilde{\boldsymbol{\xi}})\right) \,\mathrm{d}\boldsymbol{\xi}\right|.\end{aligned} \tag{18}$$

For the last term in (18) assuming, for some $\delta > 0$, $q \in H^{1+\delta}(\widehat{\Gamma}_T)$ which implies $q(\widetilde{\boldsymbol{\xi}}) \in H^{1/2+\delta}(\partial(\gamma^0\widehat{T}))$ and noting that $|\mathbf{n}_{\gamma^0\widehat{T}}| = 1$, we get

$$\begin{aligned}
&\left| \int_{\partial(\gamma^0\widehat{T})} \eta(\boldsymbol{\xi}) q(\widetilde{\boldsymbol{\xi}}) \left( \mathbf{n}_{\gamma^0\widehat{T}} \cdot \widehat{\mathbf{w}}_h(\widetilde{\boldsymbol{\xi}}) \right) \mathrm{d}\boldsymbol{\xi} \right| \\
&\qquad \leq \|q(\widetilde{\boldsymbol{\xi}})\|_{L^\infty(\partial(\gamma^0\widehat{T}))} \left( \int_{\partial(\gamma^0\widehat{T})} \eta(\boldsymbol{\xi})^2 \mathrm{d}\boldsymbol{\xi} \right)^{1/2} \left( \int_{\partial(\gamma^0\widehat{T})} \left| \widehat{\mathbf{w}}_h(\widetilde{\boldsymbol{\xi}}) \right|^2 \mathrm{d}\boldsymbol{\xi} \right)^{1/2} \\
&\qquad \lesssim \|q(\widetilde{\boldsymbol{\xi}})\|_{1/2+\delta,\partial(\gamma^0\widehat{T})} h_T^{k+5/2} \|\widehat{\mathbf{w}}_h(\widetilde{\boldsymbol{\xi}})\|_{0,\partial(\gamma^0\widehat{T})} \\
&\qquad \lesssim h_T^{k+2} \|q\|_{1+\delta,\widehat{\Gamma}_T} \|\widehat{\mathbf{w}}_h\|_{0,\widehat{\Gamma}_T} ,
\end{aligned}$$

where we have used (the one-dimensional version of) the Sobolev imbedding theorem (cf. [1, Thm. 4.12]) and the trace theorem (cf. [12, Thm. 1.5.1.2]). This allows us to deduce from (18) that

$$\begin{aligned}
\langle \widehat{\mathbf{n}} \cdot \widehat{\mathbf{v}}_h, q \rangle_{0,\widehat{\Gamma}_T} \lesssim\ & h_T^{k+2} \left( \int_{\gamma^0\widehat{T}} \left( \operatorname{div} \widehat{\mathbf{w}}_h(\widetilde{\boldsymbol{\xi}}) + \gamma_k(\widetilde{\boldsymbol{\xi}}) \right)^2 \mathrm{d}\boldsymbol{\xi} \right)^{1/2} \|q\|_{0,\widehat{\Gamma}_T} \\
&+ h_T^{k+2} \left( \int_{\gamma^0\widehat{T}} |\widehat{\mathbf{w}}_h(\widetilde{\boldsymbol{\xi}})|^2 \mathrm{d}\boldsymbol{\xi} \right)^{1/2} |q|_{1,\widehat{\Gamma}_T} \\
&+ h_T^{k+2} \left( \int_{\partial(\gamma^0\widehat{T})} |\widehat{\mathbf{w}}_h(\widetilde{\boldsymbol{\xi}})|^2 \mathrm{d}\boldsymbol{\xi} \right)^{1/2} \|q\|_{1+\delta,\widehat{\Gamma}_T}
\end{aligned} \tag{19}$$

holds. For the first term in (19) we have

$$\begin{aligned}
\operatorname{div} \widehat{\mathbf{w}}_h(\widetilde{\boldsymbol{\xi}}) + \gamma_k(\widetilde{\boldsymbol{\xi}}) = \operatorname{div} \widehat{\mathbf{w}}_h(\boldsymbol{\xi}, 0) &+ \sum_{l=1}^{k} \frac{\partial_3^l \operatorname{div} \widehat{\mathbf{w}}_h(\boldsymbol{\xi}, 0)}{l!} (\eta(\boldsymbol{\xi}))^l \\
&+ \sum_{l=0}^{k} \frac{\partial_3^{l+1} (\widehat{\mathbf{v}}_h)_3(\boldsymbol{\xi}, 0)}{(l+1)!} (\eta(\boldsymbol{\xi}))^l
\end{aligned}$$

and thus,

$$\begin{aligned}
&\int_{\gamma^0\widehat{T}} \left( \operatorname{div} \widehat{\mathbf{w}}_h(\widetilde{\boldsymbol{\xi}}) + \gamma_k(\widetilde{\boldsymbol{\xi}}) \right)^2 \mathrm{d}\boldsymbol{\xi} \lesssim \|\operatorname{div} \widehat{\mathbf{w}}_h\|_{0,\gamma^0\widehat{T}}^2 \\
&+ \int_{\gamma^0\widehat{T}} \left( (\partial_3 (\widehat{\mathbf{v}}_h)_3(\boldsymbol{\xi}, 0))^2 + \sum_{l=1}^{k} h_T^{2l(k+2)} \left( (\partial_3^l \operatorname{div} \widehat{\mathbf{w}}_h(\boldsymbol{\xi}, 0))^2 + (\partial_3^{l+1} (\widehat{\mathbf{v}}_h)_3(\boldsymbol{\xi}, 0))^2 \right) \mathrm{d}\boldsymbol{\xi} \right) \\
&\lesssim \|\operatorname{div} \widehat{\mathbf{v}}_h\|_{0,\gamma^0\widehat{T}}^2 + \sum_{l=1}^{k} h_T^{2l(k+2)} \left( \|\partial_3^l \operatorname{div} \widehat{\mathbf{w}}_h\|_{0,\gamma^0\widehat{T}}^2 + \|\partial_3^{l+1} (\widehat{\mathbf{v}}_h)_3\|_{0,\gamma^0\widehat{T}}^2 \right) \\
&\lesssim \|\operatorname{div} \widehat{\mathbf{v}}_h\|_{0,\gamma^0\widehat{T}}^2 + \sum_{l=1}^{k} h_T^{2l(k+1)-2} \|\widehat{\mathbf{v}}_h\|_{0,\gamma^0\widehat{T}}^2 \\
&\lesssim \|\operatorname{div} \widehat{\mathbf{v}}_h\|_{0,\gamma^0\widehat{T}}^2 + h_T^{2k} \|\widehat{\mathbf{v}}_h\|_{0,\gamma^0\widehat{T}}^2 \lesssim h_T^{-1} \|\operatorname{div} \widehat{\mathbf{v}}_h\|_{0,\widehat{T}}^2 + h_T^{2k-1} \|\widehat{\mathbf{v}}_h\|_{0,\widehat{T}}^2 ,
\end{aligned}$$

where inverse estimates (cf. [7, Lem. 4.5.3]) and (6) were used. For the second term in (19) we obtain

$$\int_{\gamma^0\widehat{T}} \widehat{\mathbf{w}}_h(\widetilde{\boldsymbol{\xi}})^2 \mathrm{d}\boldsymbol{\xi} \leq \|\widehat{\mathbf{v}}_h\|_{0,\widehat{\Gamma}_T}^2 \lesssim h_T^{-1} \|\widehat{\mathbf{v}}_h\|_{0,\widehat{T}}^2 .$$

Combining all this leads to

$$\langle \widehat{\mathbf{n}} \cdot \widehat{\mathbf{v}}_h, q \rangle_{0,\widehat{\Gamma}_T} \lesssim h_T^{k+3/2} \left( \|\operatorname{div} \widehat{\mathbf{v}}_h\|_{0,\widehat{T}}^2 + \|\widehat{\mathbf{v}}_h\|_{0,\widehat{T}}^2 \right)^{1/2} \|q\|_{1+\delta,\widehat{\Gamma}_T} . \tag{20}$$

Using the fact that, with $\alpha = (1+\delta)/2$, $H^\alpha(\widehat{\Gamma}_T)$ is an interpolation space of type $1/2$ between $L^2(\widehat{\Gamma}_T)$ and $H^{1+\delta}(\widehat{\Gamma}_T)$ (cf. [1, Thm. 7.23]),

$$\langle \widehat{\mathbf{n}} \cdot \widehat{\mathbf{v}}_h, q \rangle_{0,\widehat{\Gamma}_T} \lesssim h_T^{k+1} \left( \|\operatorname{div} \widehat{\mathbf{v}}_h\|_{0,\widehat{T}}^2 + \|\widehat{\mathbf{v}}_h\|_{0,\widehat{T}}^2 \right)^{1/2} \|q\|_{\alpha,\widehat{\Gamma}_T} \tag{21}$$

holds as a consequence of (17) and (20) for any $\alpha > 1/2$.

Using the fact that the definition of the parametric Raviart-Thomas elements in (2) implies that, for $\Gamma_T = F_h(\widehat{\Gamma}_T)$,

$$\langle \mathbf{n} \cdot \mathbf{v}_h, q \rangle_{0,\Gamma_T} = \langle \widehat{\mathbf{n}} \cdot \widehat{\mathbf{v}}_h, \widehat{q} \rangle_{0,\widehat{\Gamma}_T}$$

holds with a suitably scaled $\widehat{q} = \omega_T (q \circ F_h)$ (cf. [6, Lem. 2.1.6]), together with the mapping properties of $F_h$, leads to

$$\langle \mathbf{n} \cdot \mathbf{v}_h, q \rangle_{0,\Gamma_T} \lesssim h_T^{k+1} \left( \|\operatorname{div} \mathbf{v}_h\|_{0,T}^2 + \|\mathbf{v}_h\|_{0,T}^2 \right)^{1/2} \|q\|_{\alpha,\Gamma_T} . \tag{22}$$

Summing over all boundary faces,

$$\langle \mathbf{n} \cdot \mathbf{v}_h, q \rangle_{0,\Gamma} \lesssim h^{k+1} \left( \|\operatorname{div} \mathbf{v}_h\|_{0,\Omega_h}^2 + \|\mathbf{v}_h\|_{0,\Omega_h}^2 \right)^{1/2} \|q\|_{\alpha,\Gamma} \tag{23}$$

is obtained and, finally, using (7), we end up with the desired estimate (8). ∎

**4. An interpolation operator for the parametric Raviart-Thomas finite element space.** We will now construct an interpolation operator for parametric Raviart-Thomas elements which generalizes the one introduced in [3] to the case of inhomogeneous boundary conditions. Moreover, the interpolation bound below constitutes an improvement over the one in [3, Theorem 4.1] since it is stated on $\Omega$ instead of $\Omega_h$. This is required for the refined convergence analysis in the later sections.

THEOREM 2. *For the parametric Raviart-Thomas space $\mathbf{V}_h^k \subset H(\operatorname{div}, \Omega_h)$, there is an interpolation operator $\mathcal{R}_h : H(\operatorname{div}, \Omega) \cap L^s(\Omega) \to \mathbf{V}_h^k$ (with some $s > 0$, see [6, Sect. 2.5]) satisfying $\{\mathcal{R}_h \mathbf{v} : \mathbf{v} \in H_\Gamma(\operatorname{div}, \Omega)\} \subset \mathbf{V}_{h,0}^k$ such that*

$$\begin{aligned} \|\mathbf{v} - \mathcal{R}_h \mathbf{v}\|_{0,\Omega} &\lesssim h^{k+1} \|\mathbf{v}\|_{k+1,\Omega} \\ \|\operatorname{div} (\mathbf{v} - \mathcal{R}_h \mathbf{v})\|_{0,\Omega} &\lesssim h^{k+1} \|\operatorname{div} \mathbf{v}\|_{k+1,\Omega} \end{aligned} \tag{24}$$

*holds for all $\mathbf{v} \in H^{k+1}(\Omega)^d$ with $\operatorname{div} \mathbf{v} \in H^{k+1}(\Omega)$.*

Before we turn to the proof of Theorem 2, we state and prove an auxiliary result that we will repeatedly make use of. To this end, under the assumption from Theorem 1, a mapping $F : \widehat{\Omega}_h \to \Omega$ exists which inherits the smoothness and approximation properties of $\partial\Omega$, in particular,

$$\|F_h - F\|_{L^\infty(\widehat{\Omega}_h)} \lesssim h^{k+2} , \ \|J_{F_h} - J_F\|_{L^\infty(\widehat{\Omega}_h)} \lesssim h^{k+1} , \tag{25}$$

where $F_h : \widehat{\Omega}_h \to \Omega_h$ is the piecewise polynomial mapping introduced in Section 2. Furthermore,

$$\|J_F\|_{W_\infty^{k+1}(\widehat{\Omega}_h)} \lesssim 1 , \ \|J_F^{-1}\|_{W_\infty^{k+1}(\Omega)} \lesssim 1 \tag{26}$$

holds (see [7, Sect. 4.7], [15]).

LEMMA 3. *Under the assumptions from Theorem 1 on $\partial\Omega$,*

$$\|q_h \circ F_h - q_h \circ F\|_{0,\widehat{\Omega}_h} \lesssim h^{k+1} \|q_h \circ F_h\|_{0,\widehat{\Omega}_h} \tag{27}$$

*holds for all $q_h \in S_h^l$ (where the constant depends on $l \in \mathbb{N}$).*

*Proof.* The decomposition of $\widehat{\Omega}_h$ by the triangulation $\widehat{\mathcal{T}}_h$ leads to

$$\|q_h \circ F_h - q_h \circ F\|_{0,\widehat{\Omega}_h} = \left( \sum_{\widehat{T} \in \widehat{\mathcal{T}}_h} \|q_h \circ F_h - q_h \circ F\|_{0,\widehat{T}}^2 \right)^{1/2} . \tag{28}$$

For any fixed element $\widehat{T} \in \widehat{\mathcal{T}}_h$, we have, for all $\widehat{\mathbf{x}} \in \widehat{T}$, that

$$\begin{aligned} |q_h(F_h(\widehat{\mathbf{x}})) - q_h(F(\widehat{\mathbf{x}}))| &= \left| \int_0^1 \frac{d}{dt} q_h(F(\widehat{\mathbf{x}}) + t(F_h(\widehat{\mathbf{x}}) - F(\widehat{\mathbf{x}}))) \, dt \right| \\ &\leq \int_0^1 |\boldsymbol{\nabla} q_h(F(\widehat{\mathbf{x}}) + t(F_h(\widehat{\mathbf{x}}) - F(\widehat{\mathbf{x}})))| \, dt \, |F_h(\widehat{\mathbf{x}}) - F(\widehat{\mathbf{x}})| \\ &\leq |\boldsymbol{\nabla} q_h(F(\widehat{\mathbf{x}}))| \, |F_h(\widehat{\mathbf{x}}) - F(\widehat{\mathbf{x}})| + \int_0^1 t \left| \boldsymbol{\nabla}^2 q_h(\breve{\mathbf{x}}(t)) \right| \, dt \, |F_h(\widehat{\mathbf{x}}) - F(\widehat{\mathbf{x}})|^2 \end{aligned}$$

holds with $\breve{\mathbf{x}}(t) \in \operatorname{conv}(F_h(\widehat{T}) \cup F(\widehat{T}))$ for all $t \in [0,1]$. Squaring and integrating leads to

$$\begin{aligned} \|q_h \circ F_h - q_h \circ F\|_{0,\widehat{T}} &\lesssim \|(\nabla q_h) \circ F\|_{0,\widehat{T}} \|F_h - F\|_{L^\infty(\widehat{T})} \\ &\quad + \|\nabla^2 q_h\|_{L^\infty(\operatorname{conv}(F_h(\widehat{T}) \cup F(\widehat{T})))} \|F_h - F\|_{L^\infty(\widehat{T})} \|F_h - F\|_{0,\widehat{T}} \\ &\lesssim h^{k+2} \|\widehat{\nabla}(q_h \circ F_h)\|_{0,\widehat{T}} + h^{2k+4+d/2} \|\widehat{\nabla}^2 (q_h \circ F_h)\|_{L^\infty(\widehat{T})} \lesssim h^{k+1} \|q_h \circ F_h\|_{0,\widehat{T}} , \end{aligned}$$

where inverse inequalities (see [7, Theorem 4.5.11]) were used in the form

$$\|\widehat{\boldsymbol{\nabla}} \hat{q}_h\|_{0,\widehat{T}} \lesssim h^{-1} \|\hat{q}_h\|_{0,\widehat{T}} \text{ and } \|\widehat{\boldsymbol{\nabla}}^2 \hat{q}_h\|_{L^\infty(\widehat{T})} \lesssim h^{-2-\frac{d}{2}} \|\hat{q}_h\|_{0,\widehat{T}}$$

for the piecewise polynomial function $\hat{q}_h = q_h \circ F_h$. Summing over all triangles, we get from (28) the desired estimate (27). ∎

*Proof of Theorem 2.* The construction of $\mathcal{R}_h$ will be derived from the standard interpolation operator $\widehat{\mathcal{R}}_h : H(\operatorname{div}, \widehat{\Omega}_h) \cap L^s(\widehat{\Omega}_h) \to \widehat{\mathbf{V}}_h^k$ on a polyhedral domain $\widehat{\Omega}_h$ (cf. [6, Sect. 2.5]). For $\mathbf{v} \in H(\operatorname{div}, \Omega)$, we define $\widehat{\mathbf{v}} : \widehat{\Omega}_h \to \mathbb{R}^d$ by

$$\widehat{\mathbf{v}}(\widehat{\mathbf{x}}) = (\det J_F(\widehat{\mathbf{x}})) \, J_F(\widehat{\mathbf{x}})^{-1} \mathbf{v}(F(\widehat{\mathbf{x}})) \tag{29}$$

and note that $\widehat{\mathbf{v}} \in H(\operatorname{div}, \widehat{\Omega}_h)$. With respect to boundary conditions, we also have $\widehat{\mathbf{v}} \in H_{\widehat{\Gamma}_h}(\operatorname{div}, \widehat{\Omega}_h)$ if $\mathbf{v} \in H_\Gamma(\operatorname{div}, \Omega)$ (see [6, Sect. 2.1.3] for details). The interpolation operator $\mathcal{R}_h$ may now be defined for $\mathbf{x} = F_h(\widehat{\mathbf{x}}) \in \Omega_h$ by

$$(\mathcal{R}_h \mathbf{v})(F_h(\widehat{\mathbf{x}})) = \frac{1}{\det J_{F_h}(\widehat{\mathbf{x}})} J_{F_h}(\widehat{\mathbf{x}}) (\widehat{\mathcal{R}}_h \widehat{\mathbf{v}})(\widehat{\mathbf{x}}) \tag{30}$$

and extended to $\Omega$ by the piecewise polynomial representation. Since $\widehat{\mathbf{v}} \in H_{\Gamma_h}(\operatorname{div}, \Omega_h)$ implies $\widehat{\mathcal{R}}_h \widehat{\mathbf{v}} \in \widehat{\mathbf{V}}_{h,0}^k$, the same argument as above can be used to show that $\mathcal{R}_h \mathbf{v} \in \mathbf{V}_{h,0}^k$ for $\mathbf{v} \in H_\Gamma(\operatorname{div}, \Omega)$.

For the first estimate in (24) we may use the mapping $\Phi_h = F_h \circ F^{-1}$ from $\Omega$ to $\Omega_h$ (see [7, Sect. 10.4], [15]) and bound the two terms in

$$\|\mathbf{v} - \mathcal{R}_h\mathbf{v}\|_{0,\Omega} \leq \|\mathbf{v} - (\mathcal{R}_h\mathbf{v}) \circ \Phi_h\|_{0,\Omega} + \|(\mathcal{R}_h\mathbf{v}) \circ \Phi_h - \mathcal{R}_h\mathbf{v}\|_{0,\Omega} \tag{31}$$

separately. For the first term in (31), the definitions (29) and (30) lead to

$$\begin{aligned}\|\mathbf{v} - (\mathcal{R}_h\mathbf{v}) \circ \Phi_h\|_{0,\Omega} &= \left\| \left( \frac{1}{\det J_F} J_F \widehat{\mathbf{v}} - \frac{1}{\det J_{F_h}} J_{F_h} (\widehat{\mathcal{R}}_h \widehat{\mathbf{v}}) \right) (\det J_F)^{1/2} \right\|_{0,\widehat{\Omega}_h} \\ &= \left\| \frac{1}{(\det J_F)^{1/2}} J_F \left( \widehat{\mathbf{v}} - \frac{1}{\det J_{\Phi_h}} J_{\Phi_h} (\widehat{\mathcal{R}}_h \widehat{\mathbf{v}}) \right) \right\|_{0,\widehat{\Omega}_h} \lesssim \|(\det J_{\Phi_h}) J_{\Phi_h}^{-1} \widehat{\mathbf{v}} - \widehat{\mathcal{R}}_h \widehat{\mathbf{v}}\|_{0,\widehat{\Omega}_h} .\end{aligned}$$

Since $\|J_{\Phi_h} - I\|_{L^\infty(\Omega)} \lesssim h^{k+1}$ (as a consequence of (25)), this implies

$$\|\mathbf{v} - (\mathcal{R}_h\mathbf{v}) \circ \Phi_h\|_{0,\Omega} \lesssim h^{k+1} \|\widehat{\mathbf{v}}\|_{0,\widehat{\Omega}_h} + \|\widehat{\mathbf{v}} - \widehat{\mathcal{R}}_h \widehat{\mathbf{v}}\|_{0,\Omega} \lesssim h^{k+1} \|\widehat{\mathbf{v}}\|_{k+1,\widehat{\Omega}_h} , \tag{32}$$

where the interpolation estimates for the standard Raviart-Thomas elements from [6, Chp. 2.5] are used. For the second term in (31), Lemma 3 applied (component-wise) to $\mathbf{q}_h = (\widehat{\mathcal{R}}_h \widehat{\mathbf{v}}) \circ F_h^{-1}$ together with (30) gives

$$\begin{aligned}\|(\mathcal{R}_h\mathbf{v}) \circ \Phi_h - \mathcal{R}_h\mathbf{v}\|_{0,\Omega} &= \left\| \frac{1}{\det J_{F_h}} J_{F_h} \left( (\widehat{\mathcal{R}}_h \widehat{\mathbf{v}}) \circ F^{-1} - (\widehat{\mathcal{R}}_h \widehat{\mathbf{v}}) \circ F_h^{-1} \right) \right\|_{0,\Omega} \\ &\lesssim \|(\widehat{\mathcal{R}}_h \widehat{\mathbf{v}}) \circ F^{-1} - (\widehat{\mathcal{R}}_h \widehat{\mathbf{v}}) \circ F_h^{-1}\|_{0,\Omega} \\ &= \|\mathbf{q}_h \circ F_h \circ F^{-1} - \mathbf{q}_h\|_{0,\Omega} \lesssim \|\mathbf{q}_h \circ F_h - \mathbf{q}_h \circ F\|_{0,\widehat{\Omega}_h} \\ &\lesssim h^{k+1} \|\mathbf{q}_h \circ F_h\|_{0,\widehat{\Omega}_h} = h^{k+1} \|\widehat{\mathcal{R}}_h \widehat{\mathbf{v}}\|_{0,\widehat{\Omega}_h} \lesssim h^{k+1} \|\widehat{\mathbf{v}}\|_{1,\widehat{\Omega}_h} ,\end{aligned} \tag{33}$$

where the interpolation estimate for the standard Raviart-Thomas elements on $\widehat{\Omega}_h$ is used once more. The proof of the first inequality in (24) is completed by the observation that

$$\|\widehat{\mathbf{v}}\|_{k+1,\widehat{\Omega}_h} = \|(\det J_F)\, J_F^{-1} (\mathbf{v} \circ F)\|_{k+1,\widehat{\Omega}_h} \lesssim \|\mathbf{v}\|_{k+1,\Omega}$$

holds due to the transformation rules and the properties of $J_F$ in (26).

For the second inequality in (24), we start from

$$\begin{aligned}&\|\operatorname{div} \mathbf{v} - \operatorname{div} (\mathcal{R}_h\mathbf{v})\|_{0,\Omega} \\ &\quad \leq \|\operatorname{div} \mathbf{v} - (\operatorname{div} (\mathcal{R}_h\mathbf{v})) \circ \Phi_h\|_{0,\Omega} + \|(\operatorname{div} (\mathcal{R}_h\mathbf{v})) \circ \Phi_h - \operatorname{div} (\mathcal{R}_h\mathbf{v})\|_{0,\Omega} .\end{aligned} \tag{34}$$

We may bound the first term in (34) using the relations

$$\begin{aligned}\widehat{\operatorname{div}}\, \widehat{\mathbf{v}}(\widehat{\mathbf{x}}) &= (\det J_F(\widehat{\mathbf{x}}))\, (\operatorname{div} \mathbf{v})(F(\widehat{\mathbf{x}})) \\ \widehat{\operatorname{div}}\, (\widehat{\mathcal{R}}_h \widehat{\mathbf{v}})(\widehat{\mathbf{x}}) &= (\det J_{F_h}(\widehat{\mathbf{x}}))\, \operatorname{div} (\mathcal{R}_h\mathbf{v})(F_h(\widehat{\mathbf{x}}))\end{aligned}$$

which follow directly from (29) and (30), respectively (cf. [6, Sect. 2.1.3]), to obtain

$$\begin{aligned}\|\operatorname{div} \mathbf{v} - (\operatorname{div} (\mathcal{R}_h\mathbf{v})) \circ \Phi_h\|_{0,\Omega} &\lesssim \|(\operatorname{div} \mathbf{v}) \circ F - (\operatorname{div} (\mathcal{R}_h\mathbf{v})) \circ F_h\|_{0,\widehat{\Omega}_h} \\ &\leq \left\| \left( \frac{1}{\det J_F} - \frac{1}{\det J_{F_h}} \right) \widehat{\operatorname{div}}\, \widehat{\mathbf{v}} \right\|_{0,\widehat{\Omega}_h} + \left\| \frac{1}{\det J_{F_h}} \left( \widehat{\operatorname{div}}\, \widehat{\mathbf{v}} - \widehat{\operatorname{div}}\, (\widehat{\mathcal{R}}_h \widehat{\mathbf{v}}) \right) \right\|_{0,\widehat{\Omega}_h} \\ &\lesssim h^{k+1} \|\widehat{\operatorname{div}}\, \widehat{\mathbf{v}}\|_{0,\widehat{\Omega}_h} + h^{k+1} |\widehat{\operatorname{div}}\, \widehat{\mathbf{v}}|_{k+1,\widehat{\Omega}_h} \lesssim h^{k+1} \|\widehat{\operatorname{div}}\, \widehat{\mathbf{v}}\|_{k+1,\widehat{\Omega}_h} .\end{aligned}$$

The second term in (34) can be treated in a similar way as in (33) using Lemma 3 with $q_h = \widehat{\operatorname{div}}\,(\widehat{\mathcal{R}}_h\widehat{\mathbf{v}}) \circ F_h^{-1}$ and (4) which gives

(35)
$$\begin{aligned}\|(\operatorname{div}(\mathcal{R}_h\mathbf{v}))\circ\Phi_h - \operatorname{div}(\mathcal{R}_h\mathbf{v})\|_{0,\Omega} &\le \|\operatorname{div}(\mathcal{R}_h\mathbf{v})\|_{0,\Omega}\|\Phi_h - \mathrm{id}\|_{L^\infty(\Omega)}\\ &= \left\|\frac{1}{\det J_{F_h}}\left(\widehat{\operatorname{div}}(\widehat{\mathcal{R}}_h\widehat{\mathbf{v}})\circ F^{-1} - \widehat{\operatorname{div}}(\widehat{\mathcal{R}}_h\widehat{\mathbf{v}})\circ F_h^{-1}\right)\right\|_{0,\Omega}\\ &\lesssim \|\widehat{\operatorname{div}}(\widehat{\mathcal{R}}_h\widehat{\mathbf{v}})\circ F^{-1} - \widehat{\operatorname{div}}(\widehat{\mathcal{R}}_h\widehat{\mathbf{v}})\circ F_h^{-1}\|_{0,\Omega}\\ &= \|q_h\circ F_h\circ F^{-1} - q_h\|_{0,\Omega} \lesssim \|q_h\circ F_h - q_h\circ F\|_{0,\widehat{\Omega}_h}\\ &\lesssim h^{k+1}\|q_h\circ F_h\|_{0,\widehat{\Omega}_h} \lesssim h^{k+1}\|\widehat{\operatorname{div}}(\widehat{\mathcal{R}}_h\widehat{\mathbf{v}})\|_{0,\widehat{\Omega}_h} \lesssim h^{k+1}\|\widehat{\operatorname{div}}\,\widehat{\mathbf{v}}\|_{0,\widehat{\Omega}_h}\,,\end{aligned}$$

where the well-known fact was used that $\widehat{\operatorname{div}}(\widehat{\mathcal{R}}_h\widehat{\mathbf{v}}) = \widehat{\mathcal{P}}_h(\widehat{\operatorname{div}}\,\widehat{\mathbf{v}})$ with $\widehat{\mathcal{P}}_h$ being the $L^2(\widehat{\Omega})$-orthogonal projection onto $S_h^k$ (cf. [6, Prop. 2.5.2]). The proof of the second inequality in (24) is completed using the transformation rules again to obtain

$$\|\widehat{\operatorname{div}}\,\widehat{\mathbf{v}}\|_{k+1,\widehat{\Omega}_h} = \|(\det J_F)\,(\operatorname{div}\mathbf{v})\circ F\|_{k+1,\Omega} \lesssim \|\operatorname{div}\mathbf{v}\|_{k+1,\Omega}\,.$$

□

*Remark.* The second inequality in (24) implies that the interpolation operator $\mathcal{R}_h$ associated with the parametric Raviart-Thomas finite elements maps the divergence-free subspace $H^0(\operatorname{div},\Omega)$ into $\mathbf{V}_h^{k,0} := \{\mathbf{v}_h \in \mathbf{V}_h^k : \operatorname{div}\mathbf{v}_h = 0\}$. Contrary to the situation for the standard elements it is not possible to replace the norm on the right-hand side in the second line of (24) by the semi-norm. Even if $\operatorname{div}\mathbf{v}$ is indeed contained in the space $S_h^k$ defined in (5), then $\operatorname{div}(\mathcal{R}_h\mathbf{v}) \notin S_h^k$, in general.

For completeness, we also provide estimates for the projections associated with the scalar finite element space $S_h^k$ which will be needed in the later sections.

THEOREM 4. *Let the projection $\mathcal{P}_h : L^2(\Omega) \to S_h^k$ be defined by*

$$((\mathcal{P}_h p)\circ F_h, q_h\circ F_h)_{0,\widehat{\Omega}_h} = ((\det J_{\Phi_h})^{-1}(p\circ F), q_h\circ F_h)_{0,\widehat{\Omega}_h} \tag{36}$$

*for all $q_h \in S_h^k$. Then, if $p \in H^{k+1}(\Omega)$ is satisfied, the estimate*

$$\|p - \mathcal{P}_h p\|_{0,\Omega} \lesssim h^{k+1}\|p\|_{k+1,\Omega} \tag{37}$$

*holds true.*

*Proof.* Noting that (36) implies

$$(\mathcal{P}_h p)\circ F_h = \widehat{\mathcal{P}}_h((\det J_{\Phi_h})^{-1}\,(p\circ F))\,,$$

we obtain

$$\begin{aligned}\|p - \mathcal{P}_h p\|_{0,\Omega} \lesssim \|(p - \mathcal{P}_h p)\circ F\|_{0,\widehat{\Omega}_h} &\le \left\|\left(1 - (\det J_{\Phi_h})^{-1}\right)(p\circ F)\right\|_{0,\widehat{\Omega}_h}\\ &+ \left\|(\det J_{\Phi_h})^{-1}\,(p\circ F) - \widehat{\mathcal{P}}_h\left((\det J_{\Phi_h})^{-1}\,(p\circ F)\right)\right\|_{0,\widehat{\Omega}_h}\\ &+ \|(\mathcal{P}_h p)\circ F_h - (\mathcal{P}_h p)\circ F\|_{0,\widehat{\Omega}_h}\end{aligned} \tag{38}$$

and may handle the three terms separately.

For the first term in (38), we immediately get

$$\left\|\left(1 - (\det J_{\Phi_h})^{-1}\right)(p\circ F)\right\|_{0,\widehat{\Omega}_h} \lesssim h^{k+1}\|(p\circ F)\|_{0,\widehat{\Omega}_h} \lesssim h^{k+1}\|p\|_{0,\Omega}$$

using the properties (25) and (26) of $J_F$ and $J_{F_h}$. For the second term in (38), the approximation property of the standard $L^2(\widehat{\Omega})$-projection $\widehat{\mathcal{P}}_h$ together with the transformation rules and properties (26) leads to

$$\begin{aligned}\|(\det J_{\Phi_h})^{-1}(p\circ F) - \widehat{\mathcal{P}}_h\left((\det J_{\Phi_h})^{-1}(p\circ F)\right)\|_{0,\widehat{\Omega}_h}\\ \lesssim h^{k+1}\|(\det J_{\Phi_h})^{-1}\,(p\circ F)\|_{k+1,\widehat{\Omega}_h} \lesssim h^{k+1}\|p\circ F\|_{k+1,\widehat{\Omega}_h} \lesssim h^{k+1}\|p\|_{k+1,\Omega}\,.\end{aligned}$$

Finally, for the third term in (38) we may use (27) which implies

$$\begin{aligned}\|(\mathcal{P}_h p)\circ F_h - (\mathcal{P}_h p)\circ F\|_{0,\widehat{\Omega}_h} &\lesssim h^{k+1}\|\mathcal{P}_h p\|_{0,\widehat{\Omega}_h} \lesssim h^{k+1}\|(\mathcal{P}_h p)\circ F_h\|_{0,\widehat{\Omega}_h}\\ &\lesssim h^{k+1}\|\widehat{\mathcal{P}}_h\left((\det J_F)(p\circ F)\right)\|_{0,\widehat{\Omega}_h} \lesssim h^{k+1}\|(\det J_F)(p\circ F)\|_{0,\widehat{\Omega}_h}\\ &\lesssim h^{k+1}\|p\circ F\|_{0,\widehat{\Omega}_h} \lesssim h^{k+1}\|p\|_{0,\Omega}\,,\end{aligned}$$

where (26) was used repeatedly. Combining all of these estimates finishes the proof of (37). ∎

**5. Saddle point mixed formulation with parametric Raviart-Thomas elements.** We consider the use of parametric Raviart-Thomas elements in a mixed formulation of saddle point type for the Poisson equation: Find $(\mathbf{u},p)\in H_\Gamma(\mathrm{div},\Omega)\times \dot{L}^2(\Omega)$ such that

$$\begin{aligned}(\mathbf{u},\mathbf{v})_{0,\Omega} - (p,\mathrm{div}\,\mathbf{v})_{0,\Omega} &= 0\\ -(\mathrm{div}\,\mathbf{u},q)_{0,\Omega} &= -(f,q)_{0,\Omega}\end{aligned}\tag{39}$$

is satisfied for all $(\mathbf{v},q)\in H_\Gamma(\mathrm{div},\Omega)\times\dot{L}^2(\Omega)$, where the latter subspace is defined as $\dot{L}^2(\Omega)=\{q\in L^2(\Omega):(q,1)_{0,\Omega}=0\}$. For the moment, it is sufficient to assume that the right-hand side satisfies $f\in\dot{L}^2(\Omega)$. The discretized version of (39) reads as follows: Find $(\mathbf{u}_h,p_h)\in\mathbf{V}_{h,0}^k\times\dot{S}_h^k$ such that

$$\begin{aligned}(\mathbf{u}_h,\mathbf{v}_h)_{0,\Omega_h} - (p_h,\mathrm{div}\,\mathbf{v}_h)_{0,\Omega_h} &= 0\\ -(\mathrm{div}\,\mathbf{u}_h,q_h)_{0,\Omega_h} &= -(f_h,q_h)_{0,\Omega_h}\end{aligned}\tag{40}$$

holds for all $(\mathbf{v}_h,q_h)\in\mathbf{V}_{h,0}^k\times\dot{S}_h^k$ with $\dot{S}_h^k = S_h^k\cap\dot{L}^2(\Omega_h)$. For the right-hand side $f_h\in\dot{L}^2(\Omega_h)$, it is natural to use $f_h=(f\circ\Phi_h^{-1})/(\det J_{\Phi_h})$ or a sufficiently good approximation thereof. The difficulty associated with the investigation of the approximation error of (40) with respect to the exact solution defined by (39) comes from the non-conformity due to the different domains $\Omega$ and $\Omega_h$ on which the variational problems are posed. Using our estimate (8) for the normal flux in Theorem 1 allows us to derive the following result.

THEOREM 5. *Assume that, for some $k\geq 0$, the right-hand side in (39) satisfies $f\in H^{k+1}(\Omega)$ and that $\mathbf{u}\in H^{k+1}(\Omega)^d$ holds for the exact solution. Then, the (parametric) mixed finite element approximation $(\mathbf{u}_h,p_h)\in\mathbf{V}_{h,0}^k\times\dot{S}_h^k$ defined by (40) satisfies*

$$\|\mathbf{u}-\mathbf{u}_h\|_{\mathrm{div},\Omega} + \|p-p_h\|_{0,\Omega} \lesssim h^{k+1}\left(\|\mathbf{u}\|_{k+1,\Omega} + \|f\|_{k+1,\Omega}\right)\,.\tag{41}$$

*Proof.* We start with the observation that the solution $(\mathbf{u},p)\in H_\Gamma(\mathrm{div},\Omega)\times\dot{L}^2(\Omega)$ of (39) satisfies

$$(\mathbf{u},\mathbf{v}_h)_{0,\Omega} - (p,\mathrm{div}\,\mathbf{v}_h)_{0,\Omega} = (\mathbf{u}+\nabla p,\mathbf{v}_h)_{0,\Omega} - \langle p,\mathbf{n}\cdot\mathbf{v}_h\rangle_\Gamma = -\langle p,\mathbf{n}\cdot\mathbf{v}_h\rangle_\Gamma$$

for all $\mathbf{v}_h \in \mathbf{V}^k_{h,0}$. With the interpolation operators $\mathcal{R}_h : H_\Gamma(\mathrm{div},\Omega) \to \mathbf{V}^k_{h,0}$ and $\mathcal{P}_h : \dot{L}^2(\Omega) \to \dot{S}^k_h$ defined in section 4, this implies that we have

$$(\mathcal{R}_h\mathbf{u},\mathbf{v}_h)_{0,\Omega} - (\mathcal{P}_h p, \mathrm{div}\,\mathbf{v}_h)_{0,\Omega} = \sigma(\mathbf{v}_h) \qquad \text{for all } \mathbf{v}_h \in \mathbf{V}^k_{h,0} \tag{42}$$

where the functional $\sigma$ is given by

$$\sigma(\mathbf{v}_h) = (\mathcal{R}_h\mathbf{u}-\mathbf{u},\mathbf{v}_h)_{0,\Omega} - (\mathcal{P}_h p - p, \mathrm{div}\,\mathbf{v}_h)_{0,\Omega} - \langle p, \mathbf{n}\cdot\mathbf{v}_h\rangle_\Gamma\,.$$

We may now switch from $\Omega$ to $\Omega_h$ by re-writing (42) as

$$(\mathcal{R}_h\mathbf{u},\mathbf{v}_h)_{0,\Omega_h} - (\mathcal{P}_h p, \mathrm{div}\,\mathbf{v}_h)_{0,\Omega_h} = \sigma(\mathbf{v}_h) + \rho(\mathbf{v}_h) \text{ for all } \mathbf{v}_h \in \mathbf{V}^k_{h,0} \tag{43}$$

with

$$\rho(\mathbf{v}_h) = (\mathcal{R}_h\mathbf{u},\mathbf{v}_h)_{0,\Omega\setminus\Omega_h} - (\mathcal{R}_h\mathbf{u},\mathbf{v}_h)_{0,\Omega_h\setminus\Omega} - (\mathcal{P}_h p, \mathrm{div}\mathbf{v}_h)_{0,\Omega\setminus\Omega_h} + (\mathcal{P}_h p, \mathrm{div}\mathbf{v}_h)_{0,\Omega_h\setminus\Omega}.$$

Moreover, the definition of $\mathcal{R}_h$ in (30) implies

$$(\det J_{F_h})\,\mathrm{div}\,(\mathcal{R}_h\mathbf{u})\circ F_h = \widehat{\mathrm{div}}\,(\widehat{\mathcal{R}}_h\widehat{\mathbf{u}}) = \widehat{\mathcal{P}}_h(\widehat{\mathrm{div}}\,\widehat{\mathbf{u}}) = \widehat{\mathcal{P}}_h((\det J_F) f\circ F)\,, \tag{44}$$

where $\widehat{\mathcal{P}}_h$ denotes again the orthogonal projection onto $S^k_h$ with respect to $L^2(\widehat{\Omega}_h)$. Combining this with (43) and (40) leads to the system

$$\begin{aligned}(\mathcal{R}_h\mathbf{u}-\mathbf{u}_h,\mathbf{v}_h)_{0,\Omega_h} - (\mathcal{P}_h p - p_h, \mathrm{div}\,\mathbf{v}_h)_{0,\Omega_h} &= \sigma(\mathbf{v}_h) + \rho(\mathbf{v}_h)\,,\\ -(\mathrm{div}\,(\mathcal{R}_h\mathbf{u}-\mathbf{u}_h), q_h)_{0,\Omega_h} &= 0\end{aligned} \tag{45}$$

for all $\mathbf{v}_h \in \mathbf{V}^k_{h,0}$ and $q_h \in S^k_h$. The second equation in (45) is derived from (40) and (44) leading to

$$\begin{aligned}(\mathrm{div}\,\mathbf{u}_h - \mathrm{div}\,(\mathcal{R}_h\mathbf{u}), q_h)_{0,\Omega_h} &= (f_h - \frac{1}{\det J_{F_h}}\widehat{\mathcal{P}}_h((\det J_F) f\circ F)\circ F_h^{-1}, q_h)_{0,\Omega_h}\\ &= \left(\frac{1}{\det J_{F_h}}\Big((\det J_F)\, f\circ F - \widehat{\mathcal{P}}_h((\det J_F)\, f\circ F)\Big)\circ F_h^{-1}, q_h\right)_{0,\Omega_h}\\ &= \Big((\det J_F)\, f\circ F - \widehat{\mathcal{P}}_h((\det J_F)\, f\circ F), \widehat{q}_h\Big)_{0,\widehat{\Omega}_h} = 0\,.\end{aligned} \tag{46}$$

The terms on the right-hand side of the first equation in (45) may be bounded in the following way:

$$\begin{aligned}|\sigma(\mathbf{v}_h)| &\le (\|\mathbf{u}-\mathcal{R}_h\mathbf{u}\|_{0,\Omega} + \|p-\mathcal{P}_h\|_{0,\Omega})\,\|\mathbf{v}_h\|_{\mathrm{div},\Omega} + \langle p, \mathbf{n}\cdot\mathbf{v}_h\rangle\\ &\lesssim h^{k+1}\left(\|\mathbf{u}\|_{k+1,\Omega} + \|p\|_{k+1,\Omega} + \|p\|_{3/2,\Gamma}\right)\|\mathbf{v}_h\|_{\mathrm{div},\Omega}\,,\end{aligned}$$

where we have used (24), (37) and (8), and

$$\begin{aligned}|\rho(\mathbf{v}_h)| &\lesssim \frac{|\Omega\setminus\Omega_h| + |\Omega_h\setminus\Omega|}{\Omega}\left(\|\mathcal{R}_h\mathbf{u}\|_{0,\Omega}\|\mathbf{v}_h\|_{0,\Omega} + \|\mathcal{P}_h p\|_{0,\Omega}\|\mathrm{div}\,\mathbf{v}_h\|_{0,\Omega}\right)\\ &\lesssim h^{k+1}\left(\|\mathbf{u}\|_{1,\Omega} + \|p\|_{0,\Omega}\right)\|\mathbf{v}_h\|_{\mathrm{div},\Omega}\,,\end{aligned}$$

where we have used (24). Using [6, Theorem 4.2.3] the above estimates imply

$$\|\mathcal{R}_h\mathbf{u}-\mathbf{u}_h\|_{\mathrm{div},\Omega} + \|\mathcal{P}_h p - p_h\|_{0,\Omega} \lesssim h^{k+1}\left(\|\mathbf{u}\|_{k+1,\Omega} + \|p\|_{k+1,\Omega} + \|p\|_{3/2,\Gamma}\right)\,. \tag{47}$$

The proof is completed using

$$\|\mathbf{u}-\mathbf{u}_h\|_{\mathrm{div},\Omega}+\|p-p_h\|_{0,\Omega}\le\|\mathbf{u}-\mathcal{R}_h\mathbf{u}\|_{\mathrm{div},\Omega}+\|p-\mathcal{P}_hp\|_{0,\Omega}\\ +\|\mathcal{R}_h\mathbf{u}-\mathbf{u}_h\|_{\mathrm{div},\Omega}+\|\mathcal{P}_hp-p_h\|_{0,\Omega}$$

combined with (24) and (37) again and noting that, due to $\mathbf{u}=-\nabla p$, $p$ inherits the necessary regularity from $\mathbf{u}$. ∎

*Remark.* From a theoretical point of view, using the space

$$\breve{S}_h^k=\{\frac{1}{\det J_{F_h}}\widehat{q}_h\circ F_h^{-1}:\widehat{q}_h|_T \text{ polynomial of degree } k\}$$

instead of $S_h^k$ would be more satisfactory with respect to the conservation properties (cf. [16]). Since both spaces possess almost identical approximation properties for sufficiently small $h$, we work with the space $S_h^k$ which is less costly to implement.

**6. The treatment of inhomogeneous flux boundary conditions.** So far, we have restricted ourselves to homogeneous boundary conditions $\mathbf{n}\cdot\mathbf{u}=0$ on $\Gamma$ in this paper. The more general case $\mathbf{n}\cdot\mathbf{u}=g$ with $g\in H^{-1/2}(\Gamma)$ satisfying the compatibility condition

$$\langle g,1\rangle_\Gamma=(f,1)_{0,\Omega}$$

may be treated in the following way. Construct $\mathbf{u}^N\in H(\mathrm{div},\Omega)$ such that $\mathbf{n}\cdot\mathbf{u}^N=g$ and $\mathrm{div}\,\mathbf{u}^N=f$ is satisfied and set $\mathbf{u}_h^N=\mathcal{R}_h\mathbf{u}^N$. Then (39) is replaced by the problem of determining $(\mathbf{u},p)=(\mathbf{u}^N+\mathbf{u}^\circ,p)$ with $\mathbf{u}^\circ\in H_\Gamma(\mathrm{div},\Omega)$ and $p\in\dot{L}^2(\Omega)$ such that

$$\begin{aligned}(\mathbf{u}^\circ,\mathbf{v})_{0,\Omega}-(p,\mathrm{div}\,\mathbf{v})_{0,\Omega}&=-(\mathbf{u}^N,\mathbf{v})_{0,\Omega}\\ -(\mathrm{div}\,\mathbf{u},q)_{0,\Omega}&=-(f-\mathrm{div}\,\mathbf{u}^N,q)_{0,\Omega}\end{aligned}\tag{48}$$

holds for all $(\mathbf{v},q)\in H_\Gamma(\mathrm{div},\Omega)\times\dot{L}^2(\Omega)$. Similarly, the corresponding discrete problem (39) consists in finding $(\mathbf{u}_h,p_h)=(\mathbf{u}_h^N+\mathbf{u}_h^\circ,p_h)$ with $\mathbf{u}_h^\circ\in\mathbf{V}_{h,0}^k$ and $p_h\in\dot{S}_h^k$ such that

$$\begin{aligned}(\mathbf{u}_h^\circ,\mathbf{v}_h)_{0,\Omega_h}-(p_h,\mathrm{div}\,\mathbf{v}_h)_{0,\Omega_h}&=-(\mathbf{u}_h^N,\mathbf{v}_h)_{0,\Omega_h}\\ -(\mathrm{div}\,\mathbf{u}_h,q_h)_{0,\Omega_h}&=-(f_h-\mathrm{div}\,\mathbf{u}_h^N,q_h)_{0,\Omega_h}\end{aligned}\tag{49}$$

is satisfied for all $(\mathbf{v}_h,q_h)\in\mathbf{V}_{h,0}^k\times\dot{S}_h^k$.

An estimate for the approximation error which takes into account inhomogeneous boundary data can be obtained in the following way. Starting from

$$\begin{aligned}\|\mathbf{u}-\mathbf{u}_h\|_{\mathrm{div},\Omega}&\le\|\mathbf{u}^N-\mathbf{u}_h^N\|_{\mathrm{div},\Omega}+\|\mathbf{u}^\circ-\mathbf{u}_h^\circ\|_{\mathrm{div},\Omega}\\ &=\|\mathbf{u}^N-\mathcal{R}_h\mathbf{u}^N\|_{\mathrm{div},\Omega}+\|\mathbf{u}^\circ-\mathbf{u}_h^\circ\|_{\mathrm{div},\Omega}\,,\end{aligned}\tag{50}$$

we estimate the second part in a way similar to the proof of Theorem 5. Going through the steps of the proof, one observes that (45) is replaced by

$$\begin{aligned}(\mathcal{R}_h\mathbf{u}^\circ-\mathbf{u}_h^\circ,\mathbf{v}_h)_{0,\Omega_h}-(\mathcal{P}_hp-p_h,\mathrm{div}\,\mathbf{v}_h)_{0,\Omega_h}&=\sigma^\circ(\mathbf{v}_h)+\rho(\mathbf{v}_h)\,,\\ -(\mathrm{div}\,(\mathcal{R}_h\mathbf{u}-\mathbf{u}_h),q_h)_{0,\Omega_h}&=0\end{aligned}\tag{51}$$

to hold for all $\mathbf{v}_h\in\mathbf{V}_{h,0}^k$ and $q_h\in S_h^k$, where

$$\sigma^\circ(\mathbf{v}_h)=\sigma(\mathbf{v}_h)-(\mathbf{u}^N-\mathbf{u}_h^N,\mathbf{v}_h)_{0,\Omega}\,.$$

The second equation in (51) follows from (46) with $f_h$ replaced by $f_h - \operatorname{div} \mathbf{u}_h^N$ and $f$ replaced by $f - \operatorname{div} \mathbf{u}^N$. That indeed

$$\begin{aligned}(\operatorname{div} \mathbf{u}_h^N - \frac{1}{\det J_{F_h}} \widehat{\mathcal{P}}_h((\det J_F)(\operatorname{div} \mathbf{u}^N) \circ F) \circ F_h^{-1}, q_h)_{0,\Omega_h} \\ = \left( \frac{1}{\det J_{F_h}} \left( (\det J_{F_h}) \operatorname{div} (\mathcal{R}_h \mathbf{u}^N) - \widehat{\mathcal{P}}_h((\det J_F) (\operatorname{div} \mathbf{u}^N) \circ F) \circ F_h^{-1} \right), q_h \right)_{0,\Omega_h} \\ = \left( \widehat{\operatorname{div}}(\widehat{\mathcal{R}}_h \widehat{\mathbf{u}}^N) - \widehat{\mathcal{P}}_h(\widehat{\operatorname{div}}\, \widehat{\mathbf{u}}^N), \widehat{q}_h \right)_{0,\widehat{\Omega}_h} = 0\end{aligned}$$

is fulfilled for all $q_h \in S_h^k$ (with $\widehat{\mathbf{u}}^N := (\det J_F) J_F^{-1} (\mathbf{u}^N \circ F)$ and $\widehat{q}_h := q_h \circ F_h$) follows from the transformation rules (29) and (30) combined with the relation between the interpolation operator $\widehat{\mathcal{R}}_h$ and the $L^2(\widehat{\Omega}_h)$-projection $\mathcal{P}_h$.

All this means that an extra term needs to be added on the right-hand side of (41) which bounds $\|\mathbf{u}^N - \mathcal{R}_h \mathbf{u}^N\|_{\operatorname{div},\Omega}$. Theorem 2 implies

$$\begin{aligned}\|\mathbf{u}^N - \mathcal{R}_h \mathbf{u}^N\|_{\operatorname{div},\Omega} &= \|\operatorname{div} \mathbf{u}^N - \operatorname{div}(\mathcal{R}_h \mathbf{u}^N)\|_{0,\Omega} + \|\mathbf{u}^N - \mathcal{R}_h \mathbf{u}^N\|_{0,\Omega} \\ &\lesssim h^{k+1} \left( \|f\|_{k+1,\Omega} + \|\mathbf{u}^N\|_{k+1,\Omega} \right) ,\end{aligned} \tag{52}$$

which leads us to the following approximation result in the inhomogeneous case.

THEOREM 6. *Assume that, for some $k \geq 0$, the right-hand side in (48) satisfies $f \in H^{k+1}(\Omega)$, $g \in H^{k+1/2}(\Gamma)$ is satisfied for the boundary data, and that $\mathbf{u} \in H^{k+1}(\Omega)^d$ holds for the exact solution. Then, the (parametric) finite element approximation $(\mathbf{u}_h, p_h) = (\mathcal{R}_h \mathbf{u}^N + \mathbf{u}_h^\circ, p_h)$ with $(\mathbf{u}_h^\circ, p_h) \in \mathbf{V}_{h,0}^k \times \dot{S}_h^k$ defined by (49) satisfies*

$$\begin{aligned}\|\mathbf{u} - \mathbf{u}_h\|_{\operatorname{div},\Omega} + \|p - p_h\|_{0,\Omega} \\ \lesssim h^{k+1} \left( \|\mathbf{u}\|_{k+1,\Omega} + \|f\|_{k+1,\Omega} + \|g\|_{k+1/2,\Gamma} \right) .\end{aligned} \tag{53}$$

For the implementation of the method in the presence of inhomogeneous boundary conditions, a function $g_h = \mathbf{u}_h^N\big|_{\Gamma_h}$ in the trace space of $\mathbf{V}_h^k$ has to be constructed in such a way that it is consistent with $\mathbf{u}_h^N = \mathcal{R}_h \mathbf{u}^N$. To this end, we perform the steps given by (29) and (30) in the definition of the interpolation operator to the boundary values $g = \mathbf{n} \cdot \mathbf{u}^N$ on $\Gamma$ and $\mathbf{n} \cdot \mathbf{u}_h^N$ on $\Gamma_h$. We will use the transformation rules for the normal vectors

$$\mathbf{n} \circ F = \frac{J_F^{-T} \widehat{\mathbf{n}}}{\|J_F^{-T} \widehat{\mathbf{n}}\|} \text{ and } \mathbf{n} \circ F_h = \frac{J_{F_h}^{-T} \widehat{\mathbf{n}}}{\|J_{F_h}^{-T} \widehat{\mathbf{n}}\|}$$

on $\Gamma$ and $\Gamma_h$, respectively (cf. [6, Sect. 2.1]), where $\widehat{\mathbf{n}}$ denotes the (piecewise constant) outward normal on $\widehat{\Gamma}_h$. Based on the standard $L^2(\widehat{\Gamma}_h)$-orthogonal projection $\widehat{\mathcal{P}}_h^{\widehat{\Gamma}}$ onto the piecewise polynomials of degree $k$ on $\widehat{\Gamma}_h$ (the trace space of $\widehat{\mathbf{V}}_h^k$), we obtain

$$g_h = \frac{1}{(\det J_{F_h}) |J_{F_h}^{-T} \widehat{\mathbf{n}}|} \widehat{g}_h \text{ with } \widehat{g}_h = \widehat{\mathcal{P}}_h^{\widehat{\Gamma}} ((\det J_F)\, |J_F^{-T} \widehat{\mathbf{n}}|\, g) . \tag{54}$$

Since the implementation of parametric elements is carried out on the polyhedral domain $\widehat{\Omega}_h$, $\widehat{g}_h$ is what actually needs to be computed. This involves the knowledge of the mapping $F$ at least to the extent that is needed for sufficiently accurate approximation of the integrals involved in the computation of $\widehat{\mathcal{P}}_h^{\widehat{\Gamma}}$. This information needs to be extracted from the parametrization of the boundary $\Gamma$.

Before we present our computational results in order to confirm the theory of the previous sections, we need to discuss how to measure the approximation error appropriately in the absence of an explicit analytical expression for the exact solution of (39). There are several a posteriori error estimators available for this saddle point formulation, see [19, Sect. 4.8] for an overview. However, these estimators were all studied on polygonal meshes and it is beyond our scope here to investigate their behavior for the parametric case on curved boundaries. Instead we take the following more costly approach in order to assess the accuracy of our parametric finite element approximation. It goes without saying that we do not want to advertise this approach as a reasonable a posteriori error estimator to be used in practical computations.

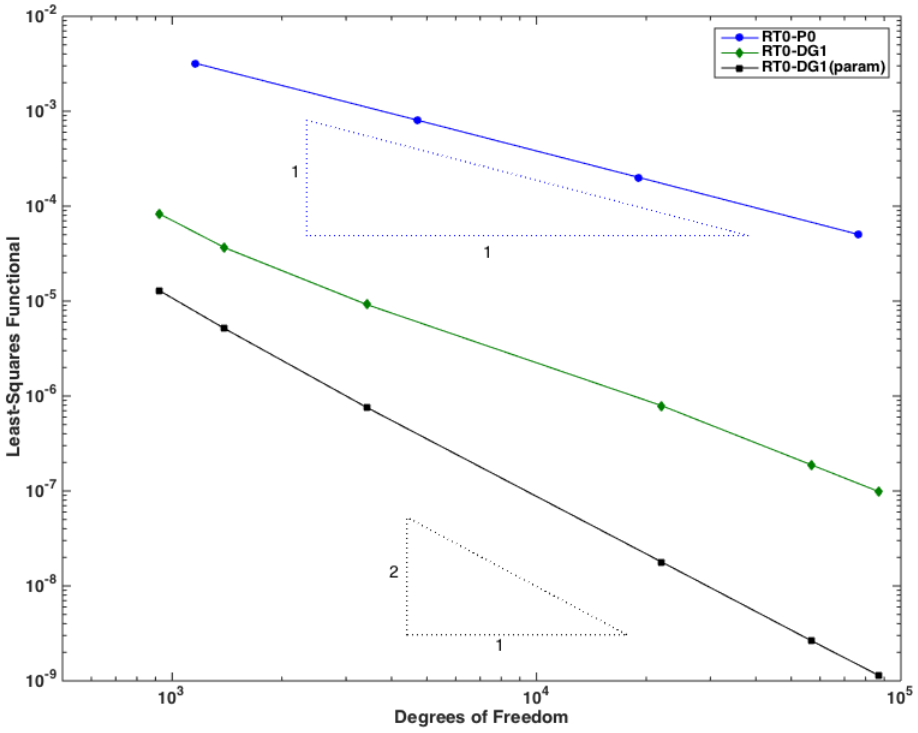


FIG. 2. *Reduction of least squares functional* $\mathcal{G}_h(\mathbf{u}_h)$ *for* $f(x_1, x_2) = \sin\, x_1$

For measuring the approximation error, we use the functional

$$\mathcal{G}_h(\mathbf{u}_h) := \inf_{q_h \in \dot{S}_h^k} \|\mathbf{u}_h + \nabla q_h\|^2_{0,\Omega_h} + \|\mathrm{div}\, \mathbf{u}_h - f_h\|^2_{0,\Omega_h}\,, \tag{55}$$

which involves the solution of the linear variational problem of finding $p_h \in \dot{S}_h^k$ such that

$$(\nabla p_h, \nabla q_h)_{0,\Omega_h} = (\mathbf{u}_h, \nabla q_h)_{0,\Omega_h} \text{ for all } q_h \in \dot{S}_h^k \tag{56}$$

holds. That this functional does in fact constitute an estimator for the approximation error of $\mathbf{u}_h$ is the statement of Proposition 7 in the appendix. Proposition 7 also

asserts that the optimal convergence order $\|\mathbf{u}-\mathbf{u}_h\|_{\mathrm{div},\Omega} \eqsim h^{k+1}$ is reached if and only if $\mathcal{G}_h(\mathbf{u}_h) \eqsim h^{2(k+1)}$. A numerical comparison of the convergence behavior for the functional and for the true error will also be presented for a simple radially symmetric problem with prescribed analytical solution.

We will now study the convergence numerically based on this quantity in order to confirm the theory presented in the previous sections. To this end, we consider (39) on the unit disk $\Omega = \{(x_1, x_2) : x_1^2 + x_2^2 < 1\}$ with boundary conditions $\mathbf{n}\cdot\mathbf{u} = 0$ on $\partial\Omega$ as in [3]. The right-hand side is chosen to be $f(x_1, x_2) = \sin(x_1)$ which, due to its symmetry, satisfies

$$\int_\Omega f\, dx = 0$$

and is therefore compatible with the boundary conditions. Alternatively, we may consider the solution $\widetilde{\mathbf{u}}$ with inhomogeneous boundary conditions $\mathbf{n}\cdot\widetilde{\mathbf{u}} = x_1\cos(x_1)$ on $\partial\Omega$ and right-hand side $\tilde{f}(x_1, x_2) \equiv 0$. It is easy to see that the solutions to these two examples are related by $\widetilde{\mathbf{u}} = \mathbf{u}^N + \mathbf{u}$ with $\mathbf{u}^N = \nabla(\sin(x_1))$.

Figure 2 shows the convergence behavior for mixed finite element approximations of different polynomial degree in terms of the functional $\mathcal{G}_h(\mathbf{u}_h)$ vs. the number of degrees of freedom $N$. The upper curve (with solid circles) illustrates a behavior of $\mathcal{G}_h(\mathbf{u}_h) \eqsim N^{-1}$ for the lowest-order case. The middle curve (with diamonds) shows the results for the combination of standard $RT_1$ spaces with discontinuous piecewise linear pressure on a polygonal approximation of $\Omega$. Obviously, the order of convergence is suboptimal in this case. Finally, the lower curve shows the optimal convergence behavior of $\mathcal{G}_h(\mathbf{u}_h) \eqsim N^{-2}$ if parametric $RT_1$ elements $\mathbf{V}^1_{h,0}$ are used instead in accordance with Theorem 5.

**Appendix. Equivalence of Functional and Error Norm.**

We state and prove the proposition concerning the equivalence of the functional (55) and the error norm.

PROPOSITION 7. *Assume that, for some $k \geq 0$, the right-hand side in (39) satisfies $f \in H^{k+1}(\Omega)$ and that $\mathbf{u} \in H^{k+1}(\Omega)$ holds for the exact solution. Then, for the (parametric) mixed finite element approximation $\mathbf{u}_h \in \mathbf{V}^k_{h,0}$ defined by (40),*

$$\|\mathbf{u}-\mathbf{u}_h\|^2_{\mathrm{div},\Omega} \lesssim \mathcal{G}_h(\mathbf{u}_h) + h^{2k+2}\|f\|^2_{k+1,\Omega} \tag{57}$$

*and*

$$\mathcal{G}_h(\mathbf{u}_h) \lesssim \|\mathbf{u}-\mathbf{u}_h\|^2_{\mathrm{div},\Omega} + h^{2k+2}\left(\|\mathbf{u}\|^2_{k+1,\Omega} + \|f\|^2_{k+1,\Omega}\right) \tag{58}$$

*holds.*

*Proof.* Due to the finite dimensionality of $\mathbf{V}^k_{h,0} \times \dot{S}^k_h$, we have that

$$\mathcal{G}_h(\mathbf{u}_h) \eqsim \inf_{q_h \in \dot{S}^k_h} \|\mathbf{u}_h + \nabla q_h\|^2_{0,\Omega} + \|\mathrm{div}\,\mathbf{u}_h - f_h\|^2_{0,\Omega} =: \mathcal{G}(\mathbf{u}_h) \tag{59}$$

holds and we may therefore prove (57) and (58) for the functional $\mathcal{G}$ instead of $\mathcal{G}_h$.

Inserting the exact solution and using the triangle inequality gives

$$\begin{aligned} \mathcal{G}(\mathbf{u}_h) &\leq \|\mathbf{u}-\mathbf{u}_h\|^2_{0,\Omega} + \inf_{p_h \in \dot{S}^k_h} \|\nabla p - \nabla p_h\|^2_{0,\Omega} + \|f - f_h\|^2_{0,\Omega} \\ &\lesssim \|\mathbf{u}-\mathbf{u}_h\|^2_{\mathrm{div},\Omega} + h^{2k+2}\left(\|\mathbf{u}\|_{k+1,\Omega} + \|f\|^2_{k+1,\Omega}\right) \end{aligned} \tag{60}$$

which proves the upper bound (58). The coercivity of the least-squares functional (cf. [5, Sect. 5.5]) implies that, for any $p_h \in \dot{S}_h^k$,

$$\begin{aligned} \|\mathbf{u}-\mathbf{u}_h\|^2_{\mathrm{div},\Omega} + \|p-p_h\|^2_{1,\Omega} &\lesssim \|\mathbf{u}-\mathbf{u}_h+\nabla(p-p_h)\|^2_{0,\Omega} + \|\mathrm{div}\,(\mathbf{u}-\mathbf{u}_h)\|^2_{0,\Omega} \\ &= \|\mathbf{u}_h+\nabla p_h\|^2_{0,\Omega} + \|f-\mathrm{div}\,\mathbf{u}_h\|^2_{0,\Omega} \end{aligned} \tag{61}$$

holds. Inserting for $p_h \in \dot{S}_h^k$ the solution of

$$(\nabla p_h, \nabla q_h)_{0,\Omega} = (\mathbf{u}_h, \nabla q_h)_{0,\Omega} \text{ for all } q_h \in \dot{S}_h^k\,,$$

(61) becomes

$$\begin{aligned} \|\mathbf{u}-\mathbf{u}_h\|^2_{\mathrm{div},\Omega} &\le \|\mathbf{u}-\mathbf{u}_h\|^2_{\mathrm{div},\Omega} + \|p-p_h\|^2_{1,\Omega} \\ &\lesssim \mathcal{G}(\mathbf{u}_h) + \|f-f_h\|_{0,\Omega} \lesssim \mathcal{G}(\mathbf{u}_h) + h^{2k+2}\|f\|^2_{k+1,\Omega} \end{aligned} \tag{62}$$

which also finishes the proof of the lower bound (57). ∎

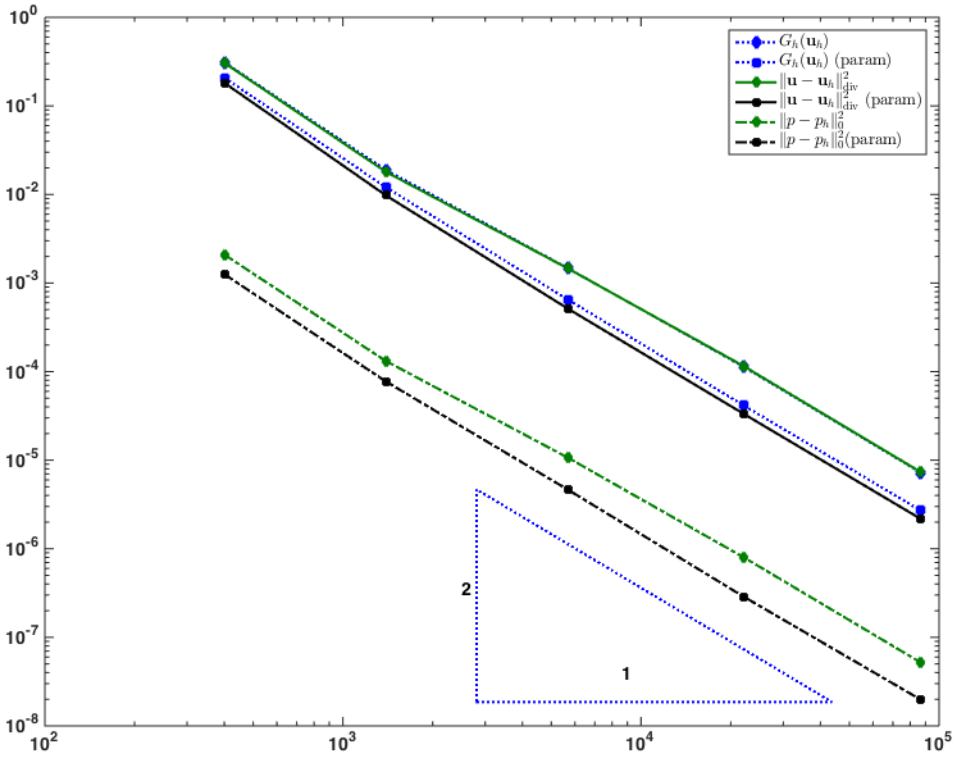


FIG. 3. *Error vs. functional for radially symmetric solution*

In order to illustrate the closeness of the functional and the actual error norm, we include a final example with a prescribed solution which we already considered in [4].

Again on the unit disk with homogeneous Neumann boundary conditions $\mathbf{n} \cdot \mathbf{u} = 0$ on $\partial\Omega$, we choose $f(x_1, x_2) = 8 - 16(x_1^2 + x_2^2)$, leading to the exact solution

$$\mathbf{u}(x_1, x_2) = \begin{pmatrix} 4x_1(1 - x_1^2 - x_2^2) \\ 4x_2(1 - x_1^2 - x_2^2) \end{pmatrix}, \; p(x_1, x_2) = (1 - x_1^2 - x_2^2)^2 - \frac{1}{3}. \tag{63}$$

Figure 3 shows that the functional $G_h(\mathbf{u}_h)$ and the $H(\mathrm{div})$ norm of the error $\mathbf{u} - \mathbf{u}_h$ are very close, both for the standard and for the parametric finite elements. In the standard case, the two lines are almost on top of each other. For such a radially symmetric problem, the deviation from the optimal order of convergence is, however, also rather hard to observe, as we have noticed before in [4] for first-order system least squares. This is not so surprising if one keeps in mind that not only $\mathbf{n} \cdot \mathbf{u}$ but the entire $\mathbf{u}$ is set to zero on the boundary, therefore leaving much less room for effects of the inexactness of the boundary conditions.

**Acknowledgement.** We are grateful to both referees for their insightful comments and suggestions.

## REFERENCES


[1] R. A. Adams and J. F. Fournier, *Sobolev Spaces*, Academic Press, New York, 2nd ed., 2003.

[2] D. N. Arnold, D. Boffi, and R. S. Falk, *Quadrilateral H(div) finite elements*, SIAM J. Numer. Anal., 42 (2005), pp. 2429–2451.

[3] F. Bertrand, S. Münzenmaier, and G. Starke, *First-order system least squares on curved boundaries: Higher-order Raviart-Thomas elements*, SIAM J. Numer. Anal., 52 (2014), pp. 3165–3180.

[4] F. Bertrand, S. Münzenmaier, and G. Starke, *First-order system least squares on curved boundaries: Lowest-order Raviart-Thomas elements*, SIAM J. Numer. Anal., 52 (2014), pp. 880–894.

[5] P. Bochev and M. Gunzburger, *Least-Squares Finite Element Methods*, Springer, New York, 2009.

[6] D. Boffi, F. Brezzi, and M. Fortin, *Mixed Finite Element Methods and Applications*, Springer, Heidelberg, 2013.

[7] S. C. Brenner and L. R. Scott, *The Mathematical Theory of Finite Element Methods*, Springer, New York, 3rd ed., 2008.

[8] Z. Cai and S. Zhang, *Robust equilibrated residual error estimator for diffusion problems: Conforming elements*, SIAM J. Numer. Anal., 50 (2012), pp. 151–170.

[9] P. G. Ciarlet, *The Finite Element Method for Elliptic Problems*, North-Holland, Amsterdam, 1978.

[10] A. Ern and M. Vohralík, *Polynomial-degree-robust a posteriori error estimates in a unified setting for conforming, nonconforming, discontinuous Galerkin, and mixed discretizations*, SIAM J. Numer. Anal., 53 (2015), pp. 1058–1081.

[11] S. Frei and T. Richter, *A locally modified parametric finite element method for interface problems*, SIAM J. Numer. Anal., 52 (2014), pp. 2315–2334.

[12] P. Grisvard, *Elliptic Problems in Nonsmooth Domains*, Pitman, Boston, 1985.

[13] A. Hannukainen, R. Stenberg, and M. Vohralik, *A unified framework for a posteriori error estimation for the Stokes equation*, Numer. Math., 122 (2012), pp. 725–769.

[14] K.-Y. Kim, *Flux reconstruction for the P2 nonconforming finite element method with application to a posteriori error estimation*, Appl. Numer. Math., 62 (2012), pp. 1701–1717.

[15] M. Lenoir, *Optimal isoparametric finite elements and error estimates for domains involving curved boundaries*, SIAM J. Numer. Anal., 23 (1986), pp. 562–580.

[16] P. J. Matuszyk and L. F. Demkowicz, *Parametric finite elements, exact sequences and perfectly matched layers*, Comput. Mech., 51 (2013), pp. 35–45.

[17] P. Monk, *Finite Element Methods for Maxwell's Equations*, Oxford University Press, New York, 2003.

[18] M. E. Rognes, R. C. Kirby, and A. Logg, *Efficient assembly of H(div) and H(curl) conforming finite elements*, SIAM J. Sci. Comput., 31 (2009), pp. 4130–4151.

[19] R. Verfürth, *A Posteriori Error Estimation Techniques for Finite Element Methods*, Oxford University Press, New York, 2013.